STATE OF OREGON
DEPARTMENT OF GEOLOGY AND MINERAL INDUSTRIES
JOHN D. BEAULIEU, STATE GEOLOGIST

# Geologic Map of the Keno Quadrangle, Klamath County, Oregon

2000

ISSN 0270-952X

## GMS-102

Geologic Map of the Keno Quadrangle, Klamath County, Oregon

By Frank R. Hladky and Stanley A. Mertzman

Supported by the U.S. Geological Survey,
Department of the Interior, under assistance
award # 98HQAG2037

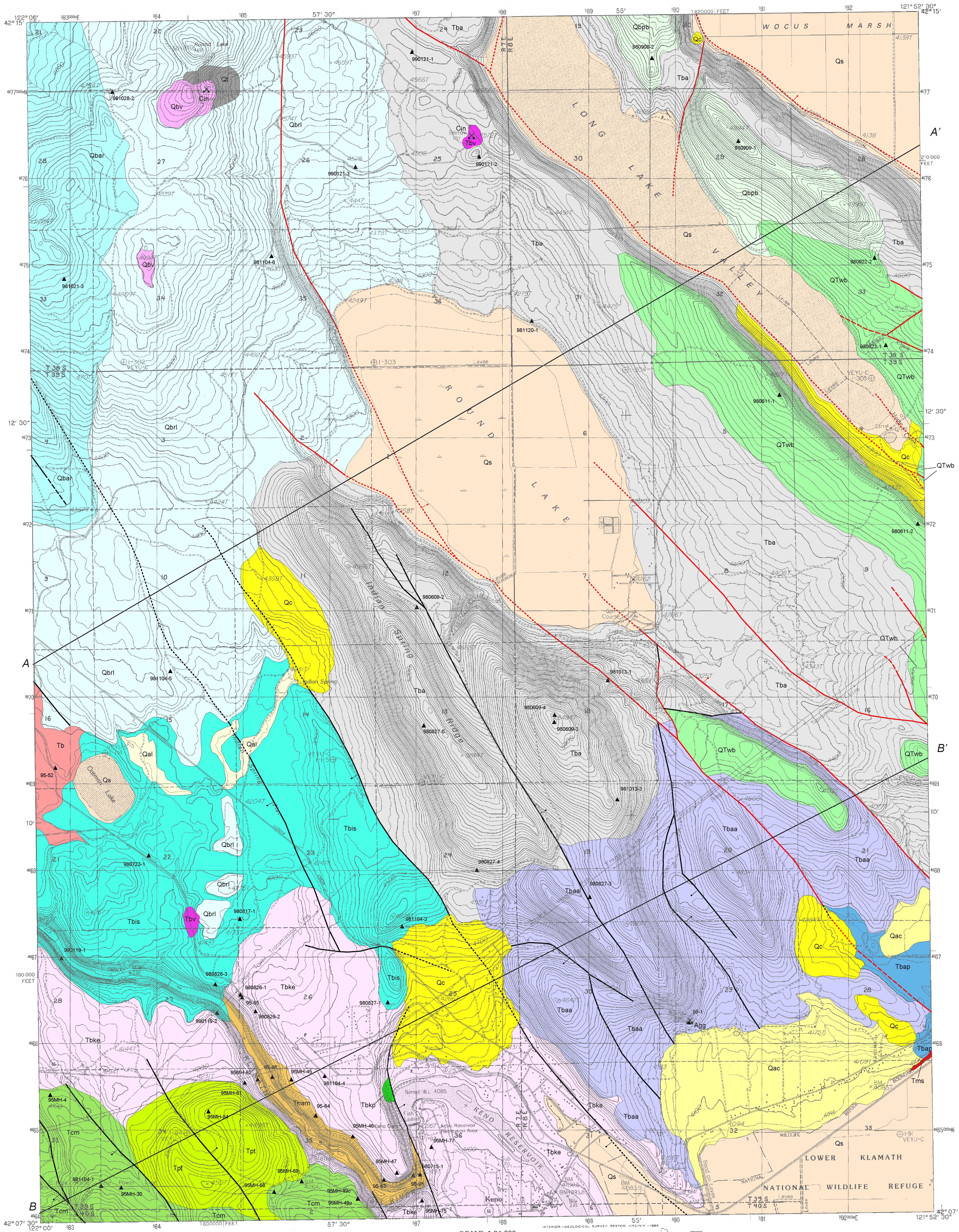

CONTROL BY ........ USGS, NOS/NOAA
COMPILED FROM AERIAL PHOTOGRAPHS TAKEN ........ 1980
FIELD CHECKED ........ 1982. MAP EDITED ........ 1985
PROJECTION ........ LAMBERT CONFORMAL CONIC
GRID: 1000-METER UNIVERSAL TRANSVERSE MERCATOR ........ ZONE 10
10,000-FOOT STATE GRID TICKS ........ OREGON, SOUTH ZONE
UTM GRID DECLINATION ........ 0°43' EAST
1980 MAGNETIC NORTH DECLINATION ........ 18° EAST
VERTICAL DATUM ... NATIONAL GEODETIC VERTICAL DATUM OF 1929
HORIZONTAL DATUM ........ 1927 NORTH AMERICAN DATUM
To place on the predicted North American Datum of 1983, move the projection lines as shown by dashed corner ticks (19 meters north / 94 meters east)
There may be private inholdings within the boundaries of any Federal and State Reservations shown on this map

SCALE 1:24 000

CONTOUR INTERVAL 20 FEET
SUPPLEMENTARY CONTOUR INTERVAL 10 FEET
CONTROL ELEVATIONS SHOWN TO THE NEAREST 0.1 FOOT
OTHER ELEVATIONS SHOWN TO THE NEAREST FOOT
To convert meters to feet multiply by 3.2808
To convert feet to meters multiply by 0.3048

QUADRANGLE LOCATION

ADJOINING 7.5' QUADRANGLE NAMES
1 Aspen Lake
2 Howard Bay
3 Wocus
4 Spencer Creek
5 Klamath Falls
6 Chicken Hills
7 Hamaker Mountain
8 Worden

INTERIOR—GEOLOGICAL SURVEY, RESTON, VIRGINIA—1986

### TIME ROCK CHART

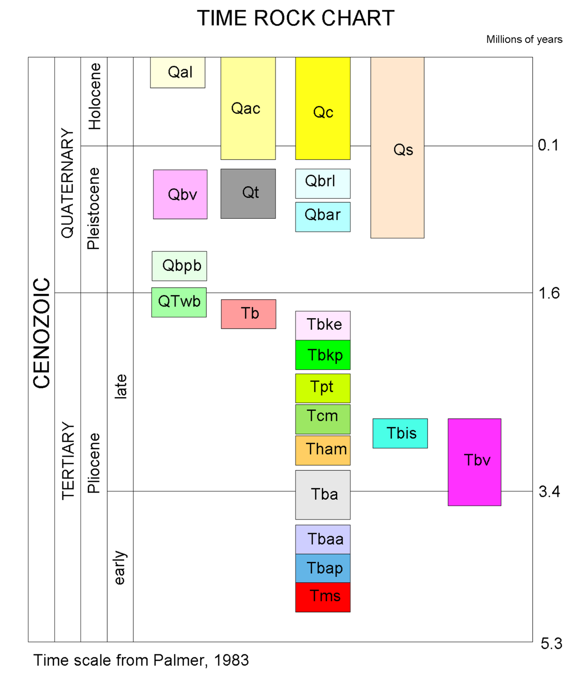


Time scale from Palmer, 1983

### MAP UNITS

**Surficial Units**

| | |
| --- | --- |
| Qal | Alluvium (Holocene) |
| Qac | Undifferentiated colluvium and alluvium (Holocene and Pleistocene) |
| Qc | Colluvium (Holocene and Pleistocene) |
| Qs | Lacustrine deposits (Holocene and Pleistocene) |

**Volcanic Units**

| | |
| --- | --- |
| Qbv | Basaltic vent deposits (Pleistocene) |
| Qt | Tuff (Pleistocene) |
| Qbrl | Basalt of Round Lake Hill (Pleistocene) |
| Qbar | Basaltic andesite of Roma (Pleistocene) |
| Qbpb | Basaltic andesite of Porter Butte (Pleistocene) |
| QTwb | Basalt of Wocus Marsh (Pleistocene or Pliocene) |
| Tb | Basalt (Pliocene) |
| Tbke | Basalt of Keno (Pliocene) |
| Tbkp | Palagonitized hyaloclastite (Pliocene) |
| Tpt | Palagonitic lapilli-ash tuff (Pliocene) |
| Tcm | Basaltic andesite of Chase Mountain (Pliocene) |
| Tbis | Basalt of Indian Spring (Pliocene) |
| Tbv | Basalt and basaltic andesite vent deposits (Pliocene) |
| Tham | Basaltic andesite of Hamaker Mountain (Pliocene) |
| Tba | Tertiary basaltic andesite (Pliocene) |
| Tbaa | Basaltic andesite augite porphyry (Pliocene) |
| Tbap | Palagonitized basaltic andesite (Pliocene) |
| Tms | Diatomaceous and tuffaceous mudstone (Pliocene) |

### GEOLOGIC MAP SYMBOLS

Contact – Approximately located

Fault – Dashed where approximately located; dotted where concealed; ball and bar on downthrown side; red where Pleistocene or younger

15 Strike and dip of bedding

15 Strike and dip of bedding – Visual field estimate

980908-2 ▲ Sample location with sample number – See numbers in Tables 1 and 2

13 Prospect, quarry, or mine with commodity type – Agg = stone, Cin = cinders

Geology by Frank R. Hladky, Oregon Department of Geology and Mineral Industries and Stanley A. Mertzman, Franklin and Marshall College

Field work conducted 1998-1999

Reviewed by David R. Sherrod, U.S. Geological Survey

### GEOLOGIC CROSS SECTIONS

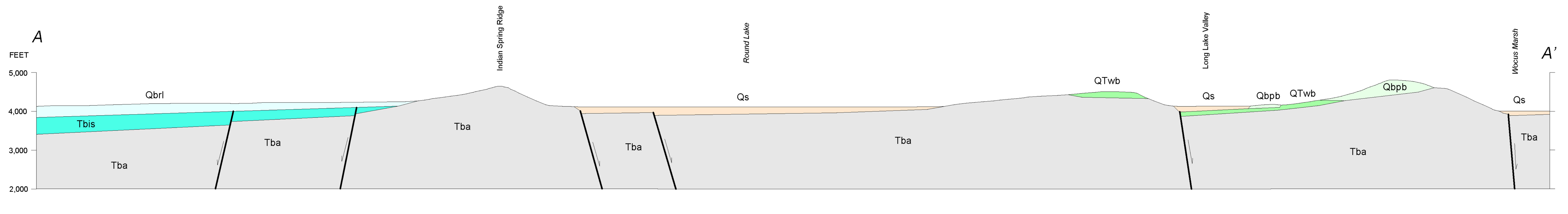


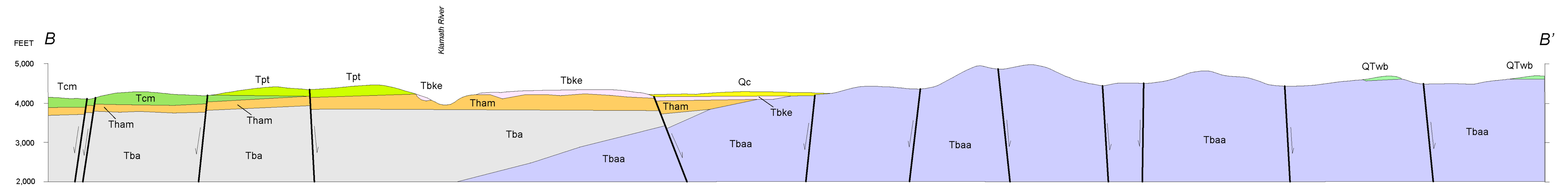

State of Oregon
Department of Geology and Mineral Industries
John D. Beaulieu, State Geologist

GMS–102
Geologic Map of the Keno Quadrangle,
Klamath County, Oregon
By F.R. Hladky and S.A. Mertzman
Text

# Geologic Map of the Keno Quadrangle, Klamath County, Oregon

*by Frank R. Hladky, Oregon Department of Geology and Mineral Industries, Grants Pass Field Office, Grants Pass, Oregon*
*and*
*Stanley A. Mertzman, Department of Geosciences, Franklin and Marshall College, Lancaster, Pennsylvania*

## INTRODUCTION

The Keno quadrangle (Figure 1) is located in southern Oregon's Klamath County, approximately 5 mi west of the city of Klamath Falls, at the juncture of the Cascade Range and Basin and Range geomorphic provinces. The northwest-trending alternation of basins and ranges is manifest across most of the quadrangle. The Klamath River flows from east to west across the grain of the topography. The valleys are typically elongate and grassy or marshy and contain ephemeral lakes. The ranges rise more than 1,000 ft above the valley floors and are typically heavily forested or recently logged. Elevations drop from 5,484 ft on Indian Spring Ridge to 3,857 ft where the Klamath River exits the quadrangle to the west. Most of the land is owned by U.S. Timberlands. The company generally allows public access but requests that visitors remove their trash and drive in a manner that will not tear up the land.

Volcanism, tectonism, and basin sedimentation are complexly interrelated. Volcanic eruptions placed basalt and basaltic andesite lavas in the quadrangle as much as 4 million years (Ma) ago and as recently as 450,000 years ago. The periodicity of lava emplacement is on the order of several hundreds of thousands of years. The chemical variance in the different lava flows and the many faults that cut them indicate that the area has been tectonically extending for at least 3 million years. Sediments in Round Lake indicate that it formed as a basin prior to 1.36 Ma. This extension goes on today, as was forcibly manifested in 1993 by a series of earthquakes that rocked the Klamath Falls area. These earthquakes occurred on the West Klamath fault zone, which has fault segments that cut through Round Lake, Long Lake Valley, and Wocus Marsh.

The Keno quadrangle is one of several 7½-minute quadrangles being mapped in the Klamath Basin, in conjunction with studies of earthquake hazards and groundwater availability conducted by various state and federal agencies. Mapping of this quadrangle was funded in part under the STATEMAP program of the U.S. Geological Survey. Data gathered during mapping have delineated geologic structures, including volcanoes and faults; identified lithologic units and given information about their geochemistry; and provided detailed age constraints for the emplacement of lavas and the formation of structures. These data are invaluable for assessing hazards and mineral and hydrologic resource potential.

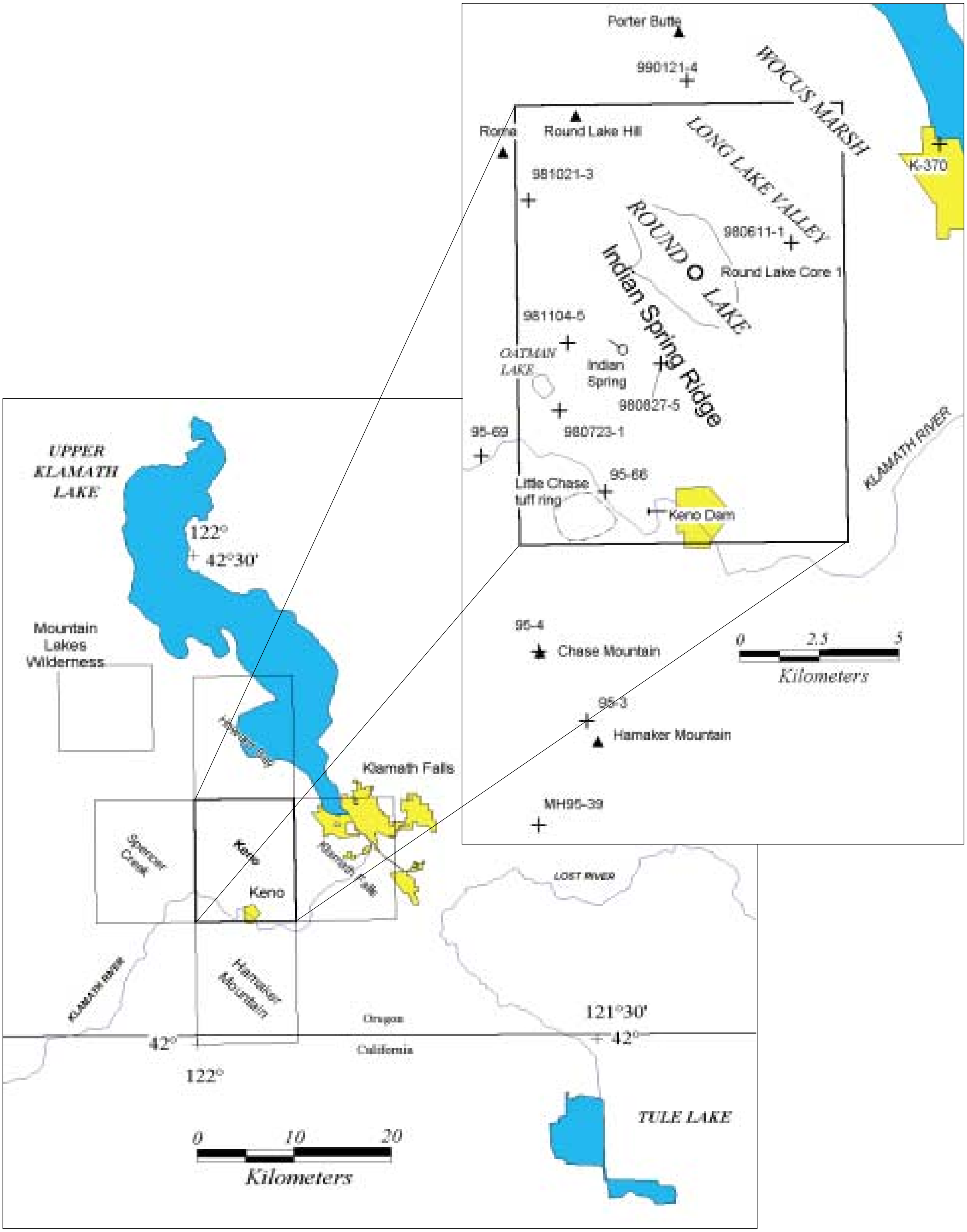


Figure 1. Location map for the Keno quadrangle and enlarged sketch map of the quadrangle and its vicinity, showing major geographic features, locations of samples ("+" sign with sample number) for which new age determinations are listed in Table 1, and the location of the drill site (open circle) where the U.S. Geological Survey obtained Round Lake Core 1.

## EXPLANATION OF MAP UNITS

### Surficial Deposits

**Qal** **Alluvium (Holocene)**—Unconsolidated gravel, sand, and silt deposited along the Indian Spring drainage (Figure 1). Thickness generally 1–3 m (3–10 ft)

**Qac** **Undifferentiated colluvium and alluvium (Holocene and Pleistocene)**—Includes (1) unconsolidated and hummocky deposits of soil and poorly sorted silt, sand, and gravel mantling bedrock slopes that are undergoing active mass movement by creep and (2) narrow, channelized deposits of moderately sorted sand and gravel from intermittent stream runoff. Found on gentle to low slopes above valley floors. Thickness generally 1–3 m (1–10 ft)

**Qc** **Colluvium (Holocene and Pleistocene)**—Unconsolidated to slightly consolidated, poorly sorted soil and fragments of bedrock displaced downslope by gravity-induced creep. May include some landslide deposits. Found on low to moderate slopes. Thickness usually a few meters but locally as much as 20 m (60 ft)

**Qs** **Lacustrine deposits (Holocene and Pleistocene)**—Unconsolidated, very light gray or white and pale pinkish tan or very light brown silty sand and silty mud. Varies from fine-grained sandy or silty units with low plasticity to highly plastic organic clays. Forms the floor of several small, enclosed basins in the quadrangle. The Klamath River in the southeast corner of the quadrangle dissects deposits of this type and age. Though generally flat lying, faulting has rotated these sediments up to 5 degrees along some basin margins near faults. Thickness generally >3 m (10 ft). Tephra from Round Lake Core 1 has been correlated with tephra ranging in age from 160 ka to 1.36 Ma (Figures 1 and 2); tephra at 49 m (160 ft) depth in Round Lake correlates with tephra from Tule Lake dated at 1.36 Ma (Adam and others, 1995). Well logs for wells in the quadrangle indicate that the greatest thicknesses are not along the Klamath River or in Long Lake Valley or Wocus Marsh but in Round Lake: up to 75 m (250 ft)

### Volcanic Units

**Qbv** **Basaltic vent deposits (Pleistocene)**—Mostly unconsolidated lapilli- and ash-sized red cinders with lesser amounts of red spatter, bombs, and scoria. These deposits are the remains of moderately eroded basaltic vent areas, in many cases cinder cones. At Round Lake Hill accumulations are up to 60 m (200 ft) thick

**Qt** **Tuff (Pleistocene)**—Pale-yellow to light-gray, moderately to poorly bedded, moderately to poorly sorted lapilli-ash and ash tuff (terminology after Dietrich and Skinner, 1979). The moderately well defined planar stratification and sorting suggest that this may be a vent surge deposit. Such deposits were erupted at Round Lake Hill and were followed by the eruption of mafic cinders and lava. Thickness about 30 m (100 ft)

**Qbrl** **Basalt of Round Lake Hill (Pleistocene)**—Orange-weathering, light- to medium-gray, slightly diktytaxitic, glomerocrystic basalt. Glomercryts (5 percent) consist of aggregate of plagioclase crystals 0.5–2 mm in diameter and are speckled with several fresh green olivine crystals (usually 0.25–1 mm across). Olivine commonly slightly iddingsitized. Olivine content about 10 percent, mostly as phenocrysts; plagioclase dominates the groundmass, making up 60–65 percent; and 25–30 percent is dark-green or black, very small (<0.1 mm) intergranular pyroxene. Flows were erupted from vents at and near Round Lake Hill. $^{40}$Ar/$^{39}$Ar age is 0.45±0.17 Ma (sample 981104–5, Table 1). Thickness variable, because unit mantled topography, but probably in excess of 120 m (400 ft)

**Qbar** **Basaltic andesite of Roma (Pleistocene)**—Orange-tan-weathering, medium-gray, fine-grained to aphanitic basaltic andesite. Contains about 4 percent fresh olivine phenocrysts (0.5–1.5 mm across) in a groundmass composed of up to 60 percent very fine (smaller than 0.1 mm), dark pyroxene and 36 percent plagioclase smaller than 0.25 mm. Texture is intergranular. Contains up to 5 percent spherical vesicles. Locally slightly diktytaxitic. Named for a summit survey marker on an unnamed knoll in the adjacent Spencer Creek quadrangle: the knoll appears to be the eroded source cone. $^{40}$Ar/$^{39}$Ar age is 0.77±0.08 Ma (sample 981021–3, Table 1). Thickness is as much as 210 m (700 ft)

**Qbpb** **Basaltic andesite of Porter Butte (Pleistocene)**—Medium-dark-gray, vesicular, seriate basalt and basaltic andesite, includes both light- and dark-colored lavas. Transparent, cola-colored iddingsitized olivine occurs as phenocrysts and groundmass grains, and dark-gray cryptocrystalline groundmass is typical. Contains about 10 percent iddingsitized olivine in a continuous range of sizes (seriate) from cryptocrytalline to 1 mm diameter. Plagioclase is also seriate and is as large as 3 mm. At least 20 percent of the rock is plagioclase larger than 0.5 mm. $^{40}Ar/^{39}Ar$ age is 1.42±0.08 Ma (sample 990121–4, Table 1). Thickness locally exceeds 210 m (700 ft)

**QTwb** **Basalt of Wocus Marsh (Pleistocene or Pliocene)**—Orange-weathering, medium-dark-gray, diktytaxitic olivine basalt. Contains 10–20 percent fine-grained (typically smaller than 0.5 mm) olivine, commonly slightly iddingsitized, especially where vesicular. Groundmass is crystalline, consisting of up to 40 percent plagioclase typically smaller than 0.25 mm, subophitically enclosed in a very fine groundmass of dark-brown, gray, and grayish-green pyroxene. Plagioclase usually projects into irregular open voids and usually not into spherical vesicles. Commonly contains rounded vesicles typically a few millimeters in diameter. Very fine grained (crystals smaller than 0.1 mm) where vesicle-rich. Where altered, the groundmass is dark olive-gray or olive black and porosity decreases to nil. Has irregular blocky fracture on a 1- to 2-m scale and forms cliffs. Geochemically similar to basalt of Keno (unit Tbke; see Table 2) but petrographically distinguished by its smaller olivine phenocrysts. $^{40}Ar/^{39}Ar$ age is 0.97±0.64 Ma on uppermost flow in adjacent Klamath Falls quadrangle (Priest, unpublished data, 1999) and 1.80±0.39 Ma this study (sample 980611–1, Table 1). Low potassium content (Priest, personal communication, 1999) and large analytical uncertainty in younger age suggest that older age is more precise. Weighted mean of the two ages is 1.58±0.33 Ma. Drapes older Tertiary units. Thickness variable; unit averages about 60 m (200 ft)

**Tb** **Basalt (Pliocene)**—Orange- and orangish-tan-weathering, medium-gray, glomerocrystic basalt. Up to 10 percent olivine smaller than 1 mm. Approximately half of all olivine is iddingsitized. Up to 25 percent of olivine, some of it iddingsitized, is glomerocrystic with plagioclase. Unit contains 15 percent plagioclase phenocrysts as large as 1.5 mm, mostly glomerocrystic with olivine. Groundmass forms 75 percent of rock; two-thirds is very fine plagioclase and one-third is dark-gray mafic (mostly pyroxene) microcrystalline material. Erupted from sources in adjacent Spencer Creek quadrangle to the west. Thickness in quadrangle typically less than 30 m (100 ft)

**Tbke** **Basalt of Keno (Pliocene)**—Medium-light-gray to medium-gray, strongly diktytaxitic olivine basalt. Olivine ranging from 1 to 3 mm constitutes 5–20 percent of rock, and some olivine is partially iddingsitized. Plagioclase smaller than 0.5 mm comprises at least 40 percent and is frequently ophitically enclosed in fine- to coarse-grained, 0.5–1.5 mm clinopyroxene and orthopyroxene that contribute up to 20 percent each. Diktytaxitic plagioclase typically projects into irregular open voids and rarely into spherical vesicles. Where partially palagonitized, the basalt loses most of its diktytaxitic texture, is dark olive gray to black and very fine grained, and in places has pillow structures. K-Ar age is 2.0±0.3 Ma (Hill, 1996). Maximum thickness about 60 m 200 ft

**Tbkp** **Palagonitized hyaloclastite (Pliocene)**—Orange, tan, and yellow palagonitized hyaloclastite consisting of loosely consolidated ash, lapilli, and blocks locally at the base of the basalt of Keno. Contains blocks of basalt of Keno that vary from nearly unaltered to thoroughly palagonitized. Grades upward into unaltered basalt. Maximum thickness 30 m (100 ft)

**Tpt** **Palagonitic lapilli-ash tuff (Pliocene)**—Mostly tan-weathering and yellowish tan, nonwelded, basaltic andesitic, lithic-vitric lapilli-ash tuff but also isolated basaltic andesite lava exposures. Tuff contains black glassy lithic fragments as large as 1 cm and gray basaltic andesite clasts (petrographically similar to unit Tcm) as large as 6 cm in a yellow palagonitic ash matrix. Deposits include Little Chase tuff ring (Figure 1) informally named by Hill (1996), an eroded and palagonitized tuff ring (Sherrod and Pickthorn, 1992; Peterson and McIntyre, 1970). Maximum thickness about 100 m (330 ft)

**Tcm** **Basaltic andesite of Chase Mountain (Pliocene)**—Poorly exposed, orangish-tan-weathering, medium-dark-gray basaltic andesite. Contains spherical vesicles (3–5 cm), up to 20 percent plagioclase phenocrysts as large as 2 mm, 20–50 percent microphenocrysts of plagioclase, 1–5 percent iddingsitized olivine (1–2 mm), 1–2 percent clinopyroxene phenocrysts as large as 0.5 mm, and 30–40 percent clinopyroxene as groundmass (<0.2 mm). Thin sections also reveal 8 percent glass and

3 percent orthopyroxene (0.05–0.8 mm). Magnetite accounts for about 3 percent. The enrichment pattern of large ion lithophile (LIL) elements is theoretically consistent with crustal contamination of an ascending basaltic magma (Hill, 1996). K-Ar age is 2.51±0.07 Ma (Hill, 1996). Maximum thickness in quadrangle about 120 m (400 ft)

**Tbis** **Basalt of Indian Spring (Pliocene)**—Medium-gray, massive, high-silica basalt. Comprises up to 15 percent microvoids <0.25 mm; 5 percent olivine <1 mm, some of which is partly iddingsitized; 10–15 percent plagioclase as phenocrysts, 1–2 mm; and 65 percent dark-gray, virtually cryptocrystalline groundmass of plagioclase, pyroxene, and traces of olivine. $^{40}Ar/^{39}Ar$ age is 2.57±0.30 Ma (sample 980723–1, Table 1). Maximum thickness is about 60 m (200 ft)

**Tbv** **Basalt and basaltic andesite vent deposits (Pliocene)**—Typically consolidated, reddish brown or reddish-gray spatter, scoria, lapilli and bomb tuff, and agglutinate. Thicknesses variable, typically <30 m (100 ft)

**Tham** **Basaltic andesite of Hamaker Mountain (Pliocene)**—Medium-brownish-gray, fine-grained, slightly porphyritic basaltic andesite. Forms ledges of tabular, poorly columnar lava flows with local 2- to 5-cm-spaced flow lamination. Exposed in map area only in Klamath River canyon; more extensive on Hamaker Mountain to the south. Contains up to 10 percent iddingsitized olivine as large as 1 mm, 1 percent orthopyroxene as large as 1 mm, and 10 percent plagioclase phenocrysts as large as 2 mm in a dark-brownish-gray, microcrystalline groundmass of plagioclase, pyroxene, and minor magnetite. Samples of unit in this study (Table 2) are basaltic andesite, basalt, and basaltic trachyandesite (when major oxides are recalculated anhydrous to 100 percent, following the IUGS recommendation of Le Bas and Streckeisen, 1991). The Hamaker Mountain lavas in the Keno quadrangle are calc-alkaline (Figure 3). The enrichment pattern of large ion lithophile (LIL) elements is theoretically consistent with crustal contamination of an ascending basaltic magma (Hill, 1996). K-Ar age is 2.72±0.19 Ma in the Keno quadrangle (Hill, 1996); similar ages are reported from the summit area and flanks of Hamaker Mountain to the south. Maximum thickness in quadrangle about 75 m (250 ft)

**Tba** **Tertiary basaltic andesite (Pliocene)**—Typically gray- or tan-weathering, dark-gray, aphanitic to porphyritic basaltic andesite. Groundmass, which forms 80–95 percent of rock, contains about 50 percent very fine plagioclase (<0.05 mm), 40 percent dark-gray cryptocrytalline material or glass, and traces of tiny (about 0.05 mm) magnetite, clinopyroxene, and olivine. Generally has a seriate texture (complete gradation from phenocryst to groundmass sizes); phenocrysts are generally plagioclase as large as 2 mm; and sporadically olivine is as large as 0.5 mm. Olivine is commonly altered to iddingsite or green earthy minerals. $^{40}Ar/^{39}Ar$ age is 4.08±0.12 Ma (sample 980827–5, Table 1). Maximum thickness about 360 m (1,200 ft)

**Tbaa** **Basaltic andesite augite porphyry (Pliocene)**—Orangish-tan- and brown-weathering, medium dark-gray to dark-greenish-gray, porphyritic basaltic andesite. Distinguished by 10 percent large (usually about 4 mm) augite phenocrysts. Also contains 5 percent pale yellowish green olivine <0.5 mm. Plagioclase phenocrysts 2–3 mm form 30–35 percent of rock. Groundmass is dark gray to dark greenish gray, very fine grained (<0.1 mm), and dominated mostly by pyroxene with subordinate plagioclase. Maximum thickness is about 300 m (1,000 ft)

**Tbap** **Palagonitized basaltic andesite (Pliocene)**—Pale- to dark-greenish-gray, significantly altered basaltic andesite exposed locally at the base of basaltic andesite augite porphyry (unit Tbaa). Typically friable, locally fragmental. Overlies unit Tms, which was probably wet at the time of lava emplacement. Maximum thickness about 10 m (30 ft)

**Tms** **Diatomaceous and tuffaceous mudstone (Pliocene)**—Pale-yellowish-greenish-gray, almost white to cream-colored diatomaceous tuffaceous mudstone. Massive and poorly bedded. Fair induration. Where deeply weathered, the unit may be only weakly indurated, locally forming a plastic silty clay with loose silty or fine sand interbeds that are difficult to distinguish from Holocene sediment of similar composition. Exposed in a low terrace in the southeast corner of the map area. Younger lacustrine deposits (unit Qs) have been deposited against the base of the terrace. Maximum exposed thickness about 10 m (30 ft)

## LANDFORM AND STRUCTURE

Straddling the border between the Cascade Range and the Basin and Range provinces, the Keno quadrangle displays volcanic landforms and tectonic structures of both. The landforms are eroded shield volcanoes and cinder cones that have been modified by faults forming horsts, grabens, and half-grabens. The constructional volcanic landforms and the faults that modify them strongly influence the region's geomorphology. The quadrangle lies astride the southern extension of the West Klamath Lake fault zone, first named by Hawkins and others (1989), on the west side of the Klamath graben (Bacon and others, 1999; Blakely and others, 1997). The West Klamath Lake fault zone is delineated by steeply dipping, down-to-the-east normal faults (Bacon and others, 1999). As originally defined, the West Klamath Lake fault zone includes the fault on the west side of Wocus Marsh. We also included similarly oriented faults along the west sides of Long Lake Valley and Round Lake. The region is tectonically active and as recently as 1993 was rocked by two large earthquakes centered 10 km northwest in the Mountain Lakes Wilderness. These earthquakes had normal-fault plane solutions and magnitudes of 5.9 and 6.0 (Wiley and others, 1993). Several hundred small-magnitude aftershocks occurred in the area over several weeks, including some centered in the Keno quadrangle (Goter, 1994). None of the 1993 earthquakes produced escarpments (Wiley and others, 1993).

The complex interplay between prehistoric volcanic effusions, extensional normal faulting, and erosion produced a collage of circular and semicircular volcanic uplands, northwest-trending ridges, and enclosed and partially enclosed basins. Older lava flows and pyroclastic strata are cut by extensional faults and covered by younger lava flows. Erosion and sedimentation have produced talus piles on steep slopes, colluvial aprons on moderate to low slopes, and lake beds in the flat basins, locally burying volcanic features and fault escarpments. Ravines and intermittent streams in many places follow faults. Incision and colluviation have blurred fault-surface traces and produced rectilinear drainage patterns on the flanks of the volcanic piles. The Klamath River has cut across the volcanic and tectonic fabric, but its course is influenced both by local fault escarpments, such as near Keno Dam, and invading lava flows.

The volcanic features consist of moderately steep-sided shield volcanoes comprised mainly of calc-alkaline lavas, low-lying shield volcanoes comprised mainly of tholeiitic lavas, and cinder cones. All lava is basalt or basaltic andesite ($SiO_2$ ranges from 47.1 to 54.8 percent). The tholeiitic lavas are typically more fluid than the calc-alkaline lavas, producing broader, smoother flows and shield morphology. Younger lavas conceal some of the earlier faults, but faulting has offset all the volcanic units. In the region, younger vents are commonly aligned along the grain of Basin and Range faults, which reflects that volcanism is influenced, to some degree, by the same tectonic strain regime as that which produces the Basin and Range topography.

Normal faults have extensively modified most volcanic features. The dominant faults strike northwest, and, as a result, most ridges trend northwest. Subordinate faults strike north-south, producing or influencing north-south-trending scarps and drainages. The few northeast- and east-west striking-faults possess small offsets.

The Tertiary basaltic andesites exposed at Indian Spring Ridge form a complex horst structure with alternating (on average) east- and west-facing normal faults. The lavas are approximately horizontal. Faulting alternates between down-to-the-east and down-to-the-west, effectively nullifying the tilting of units.

North and east of Indian Spring Ridge, dominantly tholeiitic rocks (unit QTwb) of Quaternary age drape Tertiary calc-alkaline rocks (primarily unit Tba). Although the tholeiitic rocks in turn are capped by some calc-alkaline rocks (unit Qbpb), they represent faulted volcanoes that are geomorphically shieldlike. The flanks of these shield volcanoes dip gently (<5°) to the southwest, where down-to-the-east faults dominate, producing southwest-tilted half-grabens, whose escarpments face northeast, toward the Klamath graben.

The style of faulting changes from west to east across the quadrangle. West of Round Lake, faulting has produced complex horst and graben structures. From the west side of Round Lake eastward, faulting produces west-tilted half-grabens. East of and including the Round Lake escarpment, faults dip steeply east, and offsets are down to the east. These east-dipping faults are part of the West Klamath Lake fault zone.

The offset of the basalt of Round Lake Hill (unit Qbrl) along the Round Lake escarpment indicates, with the unit's $^{40}Ar/^{39}Ar$ age of 0.45±0.17 Ma (sample 981104–5, Table 1), substantial movement along this fault of the West Klamath Lake fault zone during the last 500,000 years. West of the Round Lake escarpment, the basalt of Round Lake Hill and the basaltic andesite of Roma (unit Qbar, $^{40}Ar/^{39}Ar$ age 0.77±0.08 Ma) bury most faults. The buried faults are, in fact, west facing and are not included in the West Klamath Lake fault zone, which is part of the Klamath graben. Therefore, we can infer that the faults west of the West Klamath Lake fault zone are older, with little or no detectable offset in the last 500,000 years. Thus, it appears certain that during the Quaternary the Klamath graben faults have been tectonically more active than the faults on the Cascade Range side and, as demonstrated in 1993, are currently the tectonically most active feature in the region.

Faulting of sediment in the enclosed basins of Round Lake Valley and Long Lake, if it has occurred, is buried by the youngest deposits. Sediment at depth at Round Lake is as old as early Pleistocene, which indicates that the lake has a history dating back to at least 1.36 Ma (Adam and others, 1995). Limited well-hole data indicate that surface sediments thicken toward the center of Round Lake (Oregon Water Resources Department, 1998). Although well locations are known only imprecisely, water-well logs indicate some interfingering between thin sediment and thin lava flows in both Round Lake and Long Lake Valley. Unlike Long Lake Valley and Round Lake, Oatman Lake is not a fault-bounded feature but is bounded by lava flows.

Unit Tpt in the southwest corner of the quadrangle locates informally named Little Chase tuff ring (Figure 1), first named by Hill (1996). Peterson and McIntyre (1970) and Sherrod and Pickthorn (1992) also recognized it. This circular feature consists mainly of palagonitic tuff with a few minor lava interbeds. It formed when basaltic magma encountered ground or surface water, explosively fragmenting and altering the erupted lava.

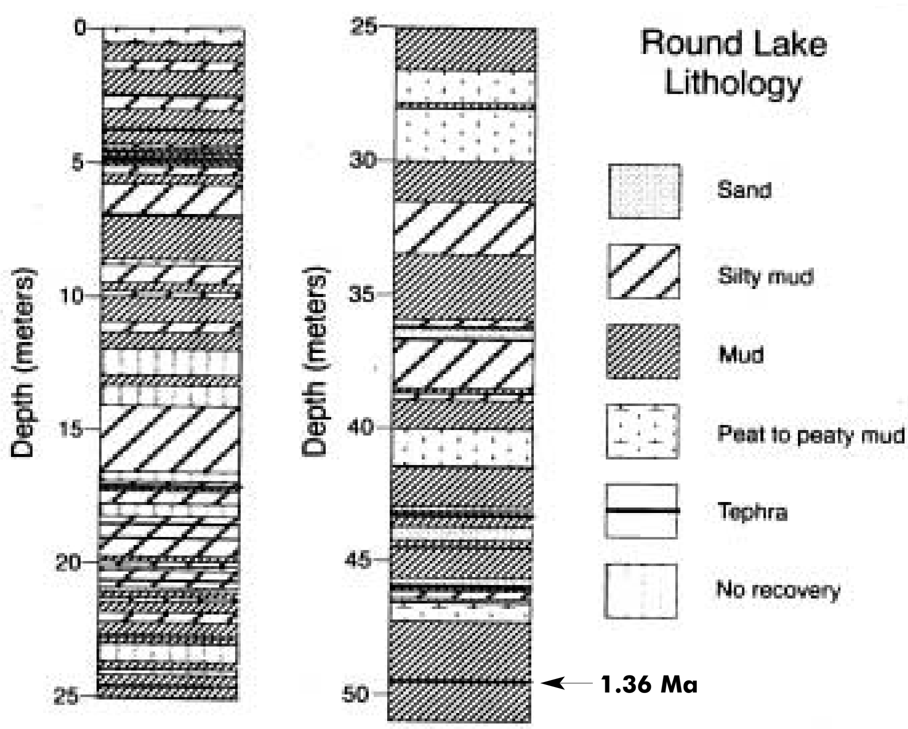


| USGS sample number | Tephra layer | Depth (m) | Age |
|---|---|---|---|
| 3469 | Paoha Island (Mono Lake) ash bed | 6.78–6.85 | 160–180 ka |
| 3475 | Rio Dell ash bed lookalike | 25.11–25.12 | 1.5 Ma |
| 3477 | Previously undescribed | 38.69–38.70 | ? |
| 3479 | May match samples 3367 and 3368 in Wocus March core | 41.30–41.33 | ? |
| 3480 | May match samples 3368, 3467, and3468 in Wocus Marsh core | 44.22–44.25 | ? |
| 3483 | Matches Sample 542 in Tule Lake core and samples 61484-45 and 61484-47 at Topsy Reservoir | 49.51–49.55 | 1.36 Ma |
| 3484 | May match samples 3367, 3467, and 3468 in Wocus Marsh core | 49.94–49.95 | <1.45 Ma |

Figure 2. Simplified lithologic log and analyses of tephra samples from Round Lake Core 1 drilled by the U.S. Geological Survey. From Adam and others (1995).

## GEOLOGIC HISTORY

The outcrops in the Keno quadrangle record a geologic history that begins no later than early Pliocene time with eruption of calc-alkaline volcanic lava related to Cascade Range volcanism. The oldest lavas include 4-Ma basaltic andesite now exposed along the deeply eroded and faulted Indian Spring Ridge. Lavas that emanated from Hamaker Mountain and Chase Mountain, two large partially eroded volcanoes to the south, are somewhat younger—about 2.5–3 Ma. The onset of Basin and Range tectonism in the quadrangle is undated, but Sherrod and Pickthorn (1992) suggest that the Klamath graben was established before 3 Ma. The historically active West Klamath Lake fault zone, which forms the western side of the Klamath graben, has produced escarpments in strata that are at least 4 Ma. Over time, Basin and Range tectonism has increasingly influenced magmatism and landscape in the quadrangle.

Calc-alkaline lavas of the Cascade Range are derived from subduction, as shown by geochemical evidence of fractionation within the crust and crustal-contamination characteristics in more evolved lavas. Tholeiitic lava, particularly high-alumina olivine tholeiite such as the basalt of Keno (unit Tbke), indicate mantle-derived, rapidly erupted (hence less evolved) lava typically found in expanding back-arc extensional terranes (Mertzman, 1996).

The oldest rocks in the quadrangle are probably mudstones (unit Tms) in the broad valley of the Klamath River. These are overlain by palagonitized lava (unit Tbap), which is, in turn, overlain by distinctive porphyritic augite lava (unit Tbaa) that crops out extensively in the southern part of Indian Spring Ridge. Palagonitic alteration, autobrecciation, and incorporation of mud in the basal lava (unit Tbap) indicate lava emplacement in a marshy or lacustrine environment. Basaltic andesite that was erupted along Indian Spring Ridge about 4 Ma includes fine-grained unit Tba (Tables 1 and 2) and chemically similar, but distinctive, coarse-grained augite porphyry (unit Tbaa, Table 2). The lavas that were erupted from this volcanic complex along Indian Spring Ridge are chemically all calc-alkaline (Figure 3).

Lavas from Hamaker Mountain to the south (unit Tham, Table 1) were erupted about 2.7 Ma (Hill, 1996). Although these lavas vary slightly in alkalinity across the basaltic andesite-basaltic trachyandesite join of Le Bas and Streckeisen (1991), they retain their calc-alkaline characteristics of rocks of the Cascade Range (Figure 3).

The eruption of the basalt of Indian Spring (unit Tbis) about 2.6 Ma (Table 1) heralds the early influence of Basin and Range tholeiitic volcanism in the quadrangle. Ferromagnesian and alkaline elements (Table 2) indicate that the Indian Spring lava is chemically transitional to tholeiitic and calc-alkaline lavas (Figure 3). Because the chemistry is transitional, extensional tectonism probably had not fully plumbed the deep magma sources for tholeiites; or the deep-sourced magmas underwent crustal contamination upon ascent, again because the extension fault system was not fully developed. The timing of this geochemical transition is roughly coincident with Sherrod and Pickthorn's (1992) estimate that the Klamath graben began about 3 Ma.

In the Cascade arc, basaltic andesite from Chase Mountain (unit Tcm) was erupted about 2.5 Ma (Hill, 1996). The lava from Chase Mountain is calc-alkaline (Table 2; Figure 3). Interbedded lava within the palagonitic tuffs (unit Tpt) of the Little Chase tuff ring are also calc-alkaline (Figure 3), indicating that this tuff ring is probably from flank eruptions along Chase Mountain, perhaps from through-going rifts (see faults on map). The 300-ft deposit of stratified palagonitic tuff at Little Chase tuff ring indicates explosive water-lava interaction. Explosive eruptions require confinement, so the lava-water interactions were occurring beneath land surface.

At about 2 Ma, the basalt of Keno (unit Tbke) was erupted. Its tholeiitic chemistry indicates that weakened, extended crust allowed the rapid ascent of mantle-derived lavas. Basin and Range faulting had traversed the Keno area by this time. Near Keno Dam, hyaloclastite (unit Tbkp) with clasts of the basalt of Keno, shows where lava flowed into a water-filled channel or small lake. The basal contact changes gradually from palagonitized to unaltered where it lies directly atop older lava from Hamaker Mountain.

The unnamed basalt of unit Tb is derived from volcanoes a few kilometers west of the map area. Chemically, it is transitional between tholeiitic and calc-alkaline (Figure 3).

The basalt of Wocus Marsh (unit QTwb) in the eastern part of the quadrangle is a low-potassium, high-alumina olivine tholeiite lava, typically light-gray, noticeably diktytaxitic, with up to 20 percent modal olivine. For the upper part of this basalt, a $^{40}Ar/^{39}Ar$ age of 0.97±0.64 Ma was determined in a sample from the adjacent Klamath Falls quadrangle (G.R. Priest, unpublished data, 1999), and a sample from the Keno quadrangle yielded an age of 1.80±0.39 Ma (Table 1). The younger sample's low potassium values and its stratigraphic relation to the basalt of Porter Butte (unit Qbpb) suggest an age of at least 1.5 Ma. The weighted mean age (ages weighed by the inverse of the variance prior to calculating the mean—standard statistical method; e.g., Taylor, 1982) of the two samples is 1.58±0.33 Ma.

Overlying the basalt of Wocus Marsh are lavas that were erupted from Porter Butte in the Howard Bay quadrangle to the north. The basaltic andesite of Porter Butte (unit Qbpb) is calc-alkaline. Erupted about 1.42±0.08 Ma (Table 1), its place in the stratigraphic sequence again demonstrates the alternating influences of Cascade Range and Basin and Range magmatism.

The stratigraphy beneath and around Round Lake from surface data and well logs indicates that the basin has been present for more than one million years. In 1991, the U.S. Geological Survey collected a single 50-m core from Round Lake (Figure 1). Age control was derived from tephra layers identified in the core. Tephra from the core ranges in age from 160 ka to 1.36 Ma (Figure 2). Tephra from core at 49 m (160 ft) depth in Round Lake correlates with tephra from Tule Lake whose age is 1.36 Ma (Adam and others, 1995), providing a minimum age for the establishment of the basin. Maximum known sediment thickness of the lacustrine deposits (unit Qs) is about 75 m (250 ft). Beneath these sediments lie lava flows. The 1.36-Ma age indicates the basin was present at the same time or shortly following the eruption of the basaltic andesite of Porter Butte. The lavas from Round Lake Hill are younger than 1 Ma and probably flowed into the basin along its northern edge. Lake sedimentation continues seasonally to the present, although much restricted because of draining and irrigation brought by civilization.

Round Lake Hill has multiple vents. The first lavas to be erupted were the calc-alkaline lavas of the basaltic andesite of Roma (unit Qbar). This unit's $^{40}Ar/^{39}Ar$ age is 0.77±0.08 Ma (Table 1). Later, as Round Lake Hill was disrupted by Basin and Range faulting, lava that was chemically transitional between calc-alkaline and tholeiitic was erupted, including the basalt of Round Lake Hill (unit Qbrl; Figure 3). The fragmental facies is shown as vent deposits (unit Qbv, primarily cinders and agglutinate) and tuff (unit Qt, cream-colored, stratified tuff). The effusive facies formed the basalt of Round Lake Hill, a fluid tholeiitic lava that flooded low spots and traveled several kilometers south. Rocks from vent areas (unit Qbv) of the basalt of Round Lake Hill show considerable vesiculation, spatter, agglutinate, and viscous flow banding. As the lava devolatilized, it became less vesicular and more fluid and flowed flatter and smoother. The basalt of Round Lake Hill is the youngest lava known in the quadrangle. It covers an older fault west of Indian Spring Ridge but is offset by faults on the west side of Round Lake. The $^{40}Ar/^{39}Ar$ age of the basalt of Round Lake Hill is 0.45±0.17 Ma (sample 981104–5, Table 1).

Since Pleistocene time, erosion has modified the volcanoes and fault scarps. Erosion, caused mostly by water and ice, has covered hillsides with colluvium, built substantial talus piles at the bases of steep slopes, deposited mud and silt as lake-bed deposits in the small enclosed basins, constructed small alluvial fans, and deposited alluvium along modern streams. Wocus Marsh, Long Lake Valley, Round Lake, and Oatman Lake are ephemeral lakes that experience infilling and sedimentation during high-runoff events, particularly in the spring. Except for Oatman Lake, all are now largely modified by agriculture. Downcutting of the Klamath River since 1 Ma has changed the hydrologic regime of the Round Lake and Long Lake Valley closed basins by lowering the regional water table. In consequence, the lakes have changed from perennial to ephemeral lakes (Adam and others, 1995).

## GEOLOGIC RESOURCES AND GEOLOGIC HAZARDS

The Keno quadrangle has moderate to high resource potential for road rock and cinders. Three existing quarries for these materials are shown on the map. Most of the cinder deposits have already been partly quarried. Crushed-rock resources are more abundant, particularly along ridge tops and in higher elevations where soil development is minimal. Diatomaceous sediments or clays are present, but those deposits lie under established agricultural land. Also, any future mineral development would undoubtedly have to consider the presence of great numbers of waterfowl, including pelicans, that frequent the area's lakes.

Numerous water wells are located in the quadrangle, particularly near the community of Keno. Groundwater resources are undoubtedly linked to the Klamath River, which is the regional discharge. Hydraulic connectivity between the Klamath River and the basins of Round Lake and Long Lake Valley has been inferred by Adam and others (1995).

The quadrangle lies about 1 km west of extensive, known geothermal resources near Klamath Falls (Oregon Department of Geology and Mineral Industries, 1982). The proximity to this geothermal zone and the presence of faults that pass from this warm zone into the Keno quadrangle indicate the possibility of finding warm subsurface waters in the Keno quadrangle. A partial inspection of well data from the quadrangle found 16°C water, or cooler than room temperature, to be the warmest water (Oregon Water Resources Department, 1998).

Quaternary faults near Klamath Falls with the potential for damaging earthquakes were delineated prior to 1993 (Hawkins and others, 1989; Sherrod and Pickthorn, 1992). The earthquake potential for the region was confirmed as residents in the Keno quadrangle experienced shaking from the earthquakes on

September 20, 1993. A foreshock with Richter magnitude 3.9 occurred at 8:16 p.m., September 20th, followed shortly after at 8:28 p.m. by a magnitude-5.9 shock and at 10:45 p.m. by a magnitude-6.0 earthquake. As many as 16 small-magnitude jolts of 2.2 to 3.8 occurred between the two main shocks (Wiley and others, 1993). Epicenters for some of the aftershocks were located in the quadrangle (Goter, 1994). Residents in Long Lake Valley reported numerous large boulder movements that accompanied the main shocks. Aftershocks continued for several months. Bacon and others (1999) report that the West Klamath Lake fault zone is capable of producing earthquakes with magnitudes ranging from 6.0 to 7.3. Faults of the West Klamath Lake fault zone pass through the northeast corner of the quadrangle. Major facilities at risk include Keno Dam, the Keno overpass, the Keno bridge over the Klamath River, high-voltage power lines, and natural-gas pipelines. The Klamath Falls region is recognized as one of Oregon's principal areas for damaging earthquakes (Madin and Mabey, 1996).

## ACKNOWLEDGMENTS

The authors would like to acknowledge the efforts of the numerous students who were funded by the Keck Foundation and worked along the Klamath River and in the Cascade Range prior to this study. Among them, Myra Hill, whose work is cited here, deserves specific recognition. We would like to express our appreciation to the many local residents who supported our work with interest and appreciation; and to Chris Sokol of U.S. Timberlands who graciously provided soil maps and access to company lands. Stanley Mertzman thanks Karen R. Mertzman for her diligent work on whole-rock analyses in the XRF lab at Franklin and Marshall College. The laboratory of Dr. Robert A. Duncan, Oregon State University, provided $^{40}Ar/^{39}Ar$ age determinations. David R. Sherrod of the U.S. Geological Survey thoroughly reviewed this document. This study was supported by the U.S. Geological Survey, Department of the Interior, under assistance award # 98HQAG2037. The views and conclusions contained in this document are those of the authors and should not be interpreted as necessarily representing the official policies, either expressed or implied, of the U.S. Government.

## REFERENCES CITED

Adam, D.P., Rieck, H.J., McGann, M.L., Schiller, K.H., and Sarna-Wojcicki, A.M., 1995, Lithologic description of a sediment core from Round Lake, Klamath County, Oregon: U.S. Geological Survey Open-File Report 95–0033, 49 p.

Bacon, C.R., Lanphere, M.A., and Champion, D.E., 1999, Late Quaternary slip rate and seismic hazards of the West Klamath Lake fault zone near Crater Lake, Oregon Cascades: Geology, v. 27, no. 1, p. 43–46.

Blakely, R.J., Christiansen, R.L., Guttanti, M., Wells, R.E., Donnelly-Nolan, J.M., Muffler, L.J.P., Clynne, M.A., and Smith, J.G., 1997, Gravity anomalies, Quaternary vents, and Quaternary faults in the southern Cascade Range, Oregon and California: Implications for arc and back-arc evolution: Journal of Geophysical Research, v. 102, p. 22,513–22,527.

Dietrich, R.V., and Skinner, B.J., 1979, Rocks and rock minerals: New York, John Wiley and Sons, 319 p.

Goter, S.K., 1994, Earthquakes in Oregon and Washington, 1872–1993: U.S. Geological Survey Open-File Report 94–226–A, scale 1:1,000,000.

Hawkins, F.F., Foley, L.L., and LaForge, R.C., 1989, Seismotectonic study for Fish Lake and Fourmile Lake Dams, Rogue River Project: U.S. Bureau of Reclamation, Denver, Colo., Geotechnical Engineering and Geology Division, Seismotectonic Report 89–3, 26 p.

Hill, M., 1996, The geochemistry and petrogenesis of volcanic rocks near Keno, Oregon, in the southern Cascade Range, *in* Manduca, C.A., and Mankiewicz, C., eds., Ninth Keck Research Symposium in Geology, abstracts volume, p. 192–195.

Irvine, T.N., and Baragar, W.R.A., 1971, A guide to the chemical classification of the common volcanic rocks: Canadian Journal of Earth Sciences, v. 8, no. 5 p. 523-548.

Le Bas, M.J., and Streckeisen, A.L., 1991, The IUGS systematics of igneous rocks: London, Journal of the Geological Society, v. 148, p. 825–833.

Madin, I.P., and Mabey, M.A., 1996, Earthquake hazard maps for Oregon: Oregon Department of Geology and Mineral Industries Geological Map Series GMS-100.

Mertzman, S.A, 1996, Late Tertiary Cascades volcanism in the area west of Klamath Falls, Oregon, *in*: Manduca, C.A., and Mankiewicz, C., eds., Ninth Keck Research Symposium in Geology, abstracts volume, p. 172–175.

Oregon Department of Geology and Mineral Industries, 1982, Geothermal resources of Oregon, 1982: National Oceanic and Atmospheric Administration (for U.S. Department of Energy), scale 1:500,000.

Oregon Water Resources Department, 1998, GRID: Groundwater resource information distribution, south-central Oregon, Klamath and Lake Counties, May 1998, CD-ROM, 2 disks.

Palmer, A.R., 1983, The decade of North American Geology 1983 geologic time scale: Geology, v. 11, no. 9, p. 503–504.

Peterson, N.V., and McIntyre, J.R., 1970, The reconnaissance geology and mineral resources of eastern Klamath County and western Lake County, Oregon: Oregon Department of Geology and Mineral Industries Bulletin 66, 70 p.

Sherrod, D.R., and Pickthorn, L.B.G., 1992, Geologic map of the west half of the Klamath Falls 1° by 2° quadrangle, south-central Oregon: U.S. Geological Survey Miscellaneous Investigations Series Map I–2182, scale 1:250,000.

Taylor, J.R., 1982, An introduction to error analysis: Mill Valley, Calif., University Science Books, 270 p.

Wiley, T.J., Sherrod, D.R., Keefer, D.K., Qamar, A., Schuster, R.L., Dewey, J.W., Mabey, M.A., Black, G.L., and Wells, R.E., 1993, Klamath Falls earthquakes, September 20, 1993-including the strongest quake ever measured in Oregon: Oregon Geology, v. 55, no. 6, p. 127–134.

Table 1. New isotopic whole-rock ages for samples from the Keno quadrangle and adjoining quadrangles. K-Ar ages provided by S.A. Mertzman. $^{40}Ar/^{39}Ar$ ages provided by R.A. Duncan, Oregon State University. Locations shown on Figure 1. E = x10; na = not applicable. Eastings and northings referable to 1927 North American datum, zone 10.

| Sample no. | ¼ | ¼ | Sec. | T.(S.) | R.(E.) | UTM N | UTM E | Quadrangle | Unit | Lithology | Method | Wt. % $K_2O$ | $^{40}Ar_{rad}$ /gm | $\%^{40}Ar_{rad}$ | First reported | Age (Ma) |
|---|---|---|---|---|---|---|---|---|---|---|---|---|---|---|---|---|
| 981104-5 | NW | NE | 15 | 39 | 7 | 4670300 | 584160 | Keno | Qbrl | Basalt | $^{40}Ar/^{39}Ar$ | na | na | na | This study | 0.45±0.17 |
| 981021-3 | SE | NE | 33 | 38 | 7 | 4674835 | 582930 | Keno | Qbar | Basaltic andesite | $^{40}Ar/^{39}Ar$ | na | na | na | This study | 0.77±0.08 |
| K-370 | SE | NW | 26 | 38 | 8 | 4676500 | 595900 | Klamath Falls | QTwb | Basalt | $^{40}Ar/^{39}Ar$ | na | na | na | Priest | 0.97±0.64 |
| 990121-4 | NE | NE | 24 | 38 | 7 | 4678615 | 587925 | Howard Bay | Qbpb | Basaltic andesite | $^{40}Ar/^{39}Ar$ | na | na | na | This study | 1.42±0.08 |
| 980611-1 | NE | NE | 5 | 39 | 8 | 4673495 | 591205 | Keno | QTwb | Basalt | $^{40}Ar/^{39}Ar$ | na | na | na | This study | 1.80±0.39 |
| 95-69 | SE | NE | 29 | 39 | 7 | 4666740 | 581460 | Spencer Creek | Tbke | Basalt | K-Ar | 0.13 | 3.703E-13 | 6.00 | Hill, 1996 | 2.0±0.3 |
| 95-4 | NE | NE | 16 | 40 | 7 | 4660560 | 583260 | Hamaker Mtn. | Tcm | Basaltic andesite | K-Ar | 1.22 | 4.408E-12 | 53.28 | Hill, 1996 | 2.51±0.07 |
| 980723-1 | SE | NW | 22 | 39 | 7 | 4668170 | 583910 | Keno | Tbis | Basalt | $^{40}Ar/^{39}Ar$ | na | na | na | This study | 2.57±0.30 |
| 95-66 | NW | NW | 35 | 39 | 7 | 4665610 | 585340 | Keno | Tham | Basaltic trachy-andesite | K-Ar | 1.35 | 5.29E-12 | 23.26 | Hill, 1996 | 2.72±0.19 |
| MH95-39 | NE | SE | 33 | 40 | 7 | 4655080 | 583260 | Hamaker Mtn. | Tham | Basaltic andesite | K-Ar | 1.74 | 7.227E-12 | 27.33 | This study | 2.88±0.17 |
| 95-3 | NE | SE | 22 | 40 | 7 | 4658360 | 584770 | Hamaker Mtn. | Tham | Basaltic andesite | K-Ar | 1.01 | 4.314E-12 | 20.62 | This study | 2.96±0.17 |
| 980827-5 | NE | SW | 13 | 39 | 7 | 4669670 | 587090 | Keno | Tba | Basaltic andesite | $^{40}Ar/^{39}Ar$ | na | na | na | This study | 4.08±0.12 |

Next two pages →

Figure 3. Tholeiitic and calc-alkaline characteristics of rocks in the Keno quadrangle by unit, using the AFM diagram of Irvine and Baragar (1971).

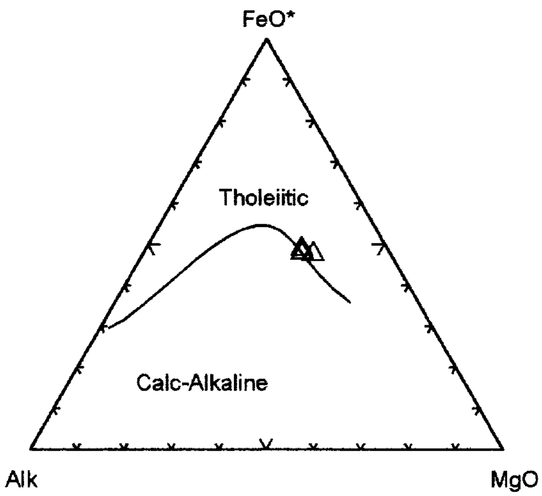


Unit Qbrl
0.45±0.17 Ma

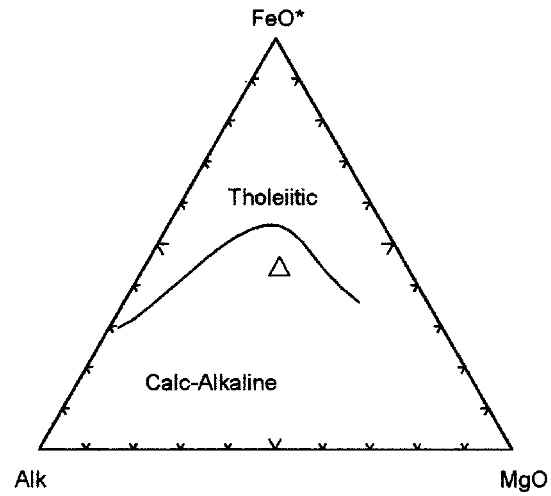


Unit Qbar
0.77±0.08 Ma

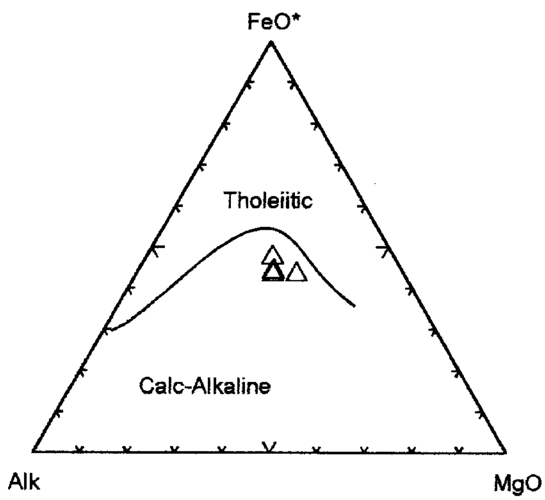


Unit Qbpb
1.42±0.08 Ma

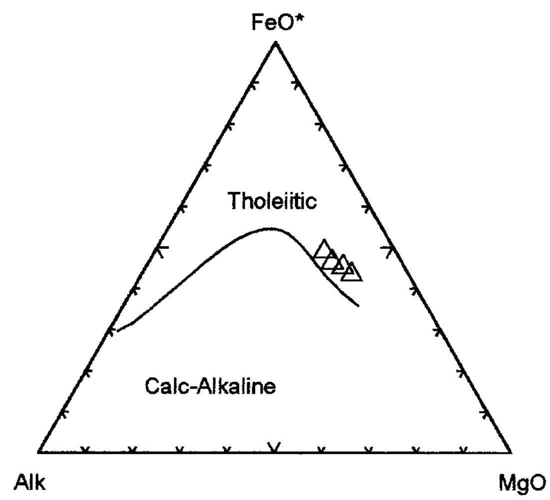


Unit QTwb
1.80±0.39 Ma

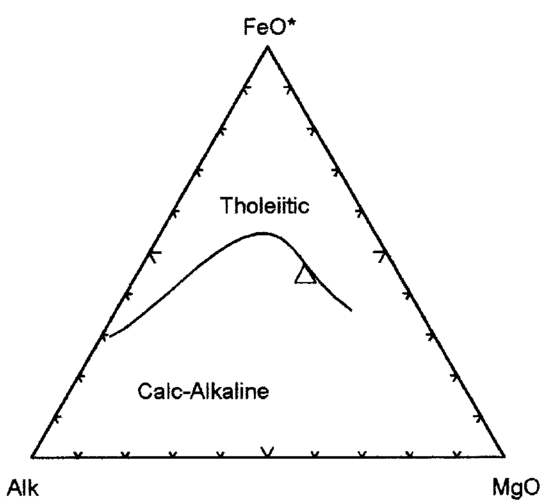


Unit Tb
(no isotopic age)

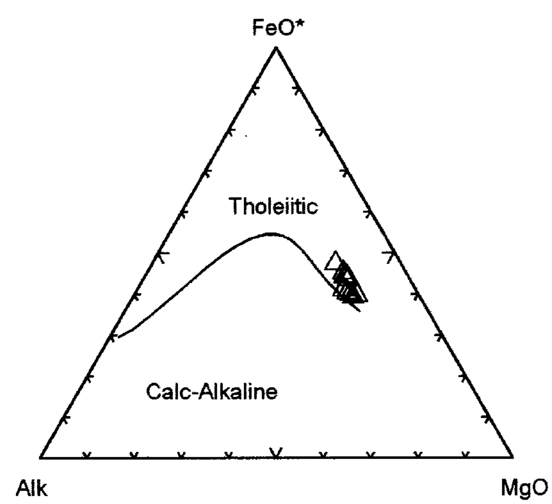


Unit Tbke
2.0±0.3 Ma

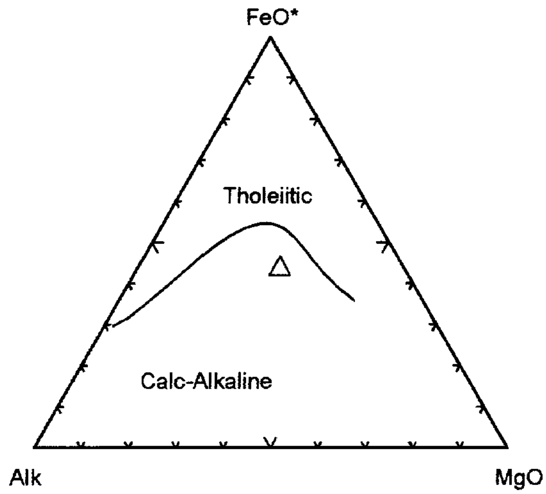


Unit Tpt
(no isotopic age)

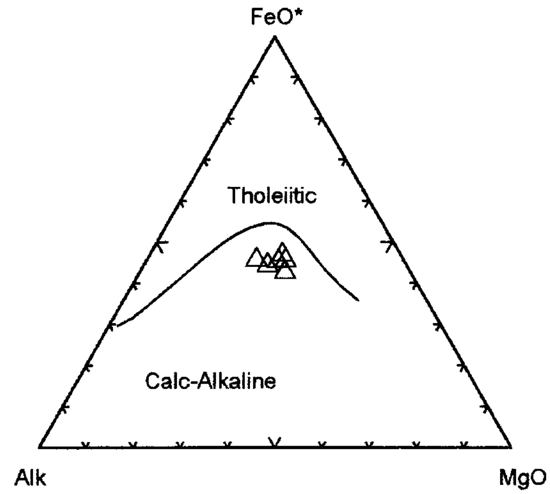


Unit Tcm
2.51±0.07 Ma

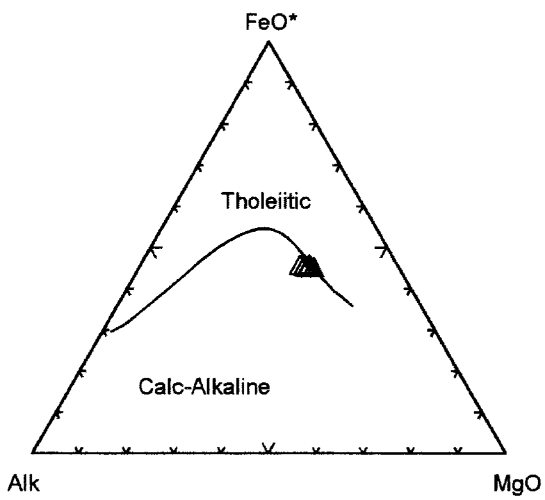


Unit Tbis
2.57±0.30 Ma

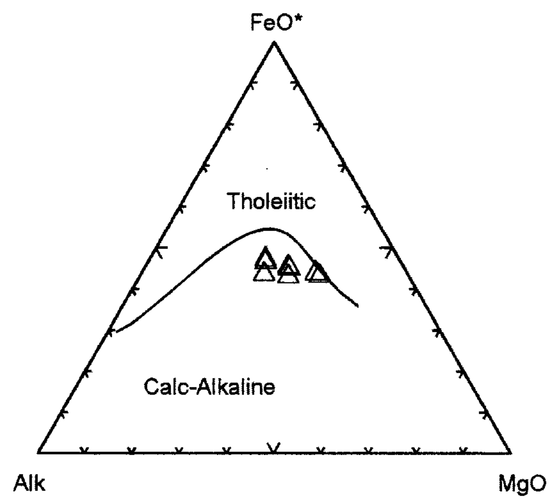


Unit Tham
2.72±0.19 Ma

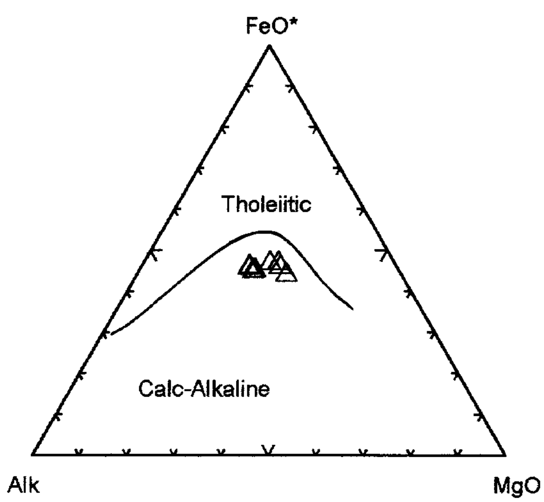


Unit Tba
4.08±0.12 Ma

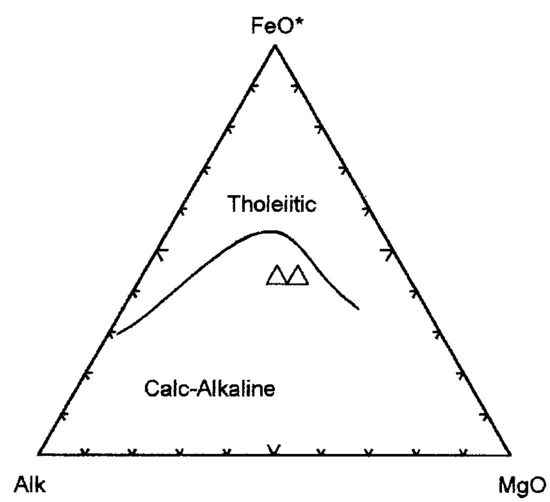


Unit Tbaa
(no isotopic age)

Table 2. Whole-rock analyses sorted by rock unit, Keno quadrangle*, Klamath County, Oregon. Major oxides reported in weight ➝
shall College, Lancaster, Pennsylvania. Note that table extends across two pages.

| Sample no. | ¼ | ¼ | Sec. | T.(S.) | R.(E.) | UTM N | UTM E | Unit | Lithology | $SiO_2$ | $TiO_2$ | $Al_2O_3$ | $Fe_2O_3$ | FeO | MnO | MgO | CaO | $Na_2O$ | $K_2O$ | $P_2O_5$ | LOI | Total |
|---|---|---|---|---|---|---|---|---|---|---|---|---|---|---|---|---|---|---|---|---|---|---|
| 981028-2 | NW | NW | 27 | 38 | 7 | 4677000 | 583490 | Qbrl | Basalt | 48.68 | 1.47 | 16.84 | 2.53 | 8.12 | 0.18 | 7.93 | 9.25 | 3.25 | 0.33 | 0.23 | 0.62 | 99.43 |
| 981104-5 | NW | NE | 15 | 39 | 7 | 4670300 | 584160 | Qbrl | Basalt | 49.28 | 1.58 | 17.48 | 2.03 | 7.99 | 0.17 | 6.91 | 9.55 | 3.34 | 0.47 | 0.33 | 0.65 | 99.78 |
| 981104-6 | NE | NW | 35 | 38 | 7 | 4675100 | 585330 | Qbrl | Basalt | 48.59 | 1.58 | 17.71 | 2.87 | 7.22 | 0.17 | 6.91 | 8.99 | 3.28 | 0.45 | 0.33 | 1.30 | 99.40 |
| 990121-3 | NE | SE | 26 | 38 | 8 | 4676130 | 586300 | Qbrl | Basalt | 48.82 | 1.62 | 17.44 | 3.29 | 7.22 | 0.18 | 6.95 | 8.79 | 3.26 | 0.53 | 0.35 | 1.35 | 99.80 |
| 981021-3 | SE | NE | 33 | 38 | 7 | 4674835 | 582930 | Qbar | Basaltic andesite | 53.99 | 0.93 | 18.10 | 2.33 | 5.34 | 0.13 | 4.95 | 7.84 | 3.63 | 1.00 | 0.26 | 0.79 | 99.29 |
| 990121-4* | NE | NE | 24 | 38 | 7 | 4678615 | 587925 | Qbpb | Basaltic andesite | 54.44 | 0.91 | 18.37 | 1.98 | 5.62 | 0.13 | 4.86 | 7.86 | 3.68 | 0.93 | 0.26 | 0.91 | 99.95 |
| 990125-1* | NE | NE | 24 | 38 | 7 | 4678615 | 587925 | Qbpb | Basaltic andesite | 54.59 | 0.90 | 18.03 | 1.65 | 5.78 | 0.13 | 4.89 | 7.75 | 3.66 | 1.01 | 0.26 | 0.87 | 99.52 |
| 980908-2 | SW | SW | 20 | 38 | 8 | 4677390 | 589730 | Qbpb | Basaltic andesite | 52.21 | 0.99 | 17.38 | 4.49 | 4.14 | 0.15 | 6.46 | 8.51 | 3.66 | 0.67 | 0.24 | 0.91 | 99.81 |
| 980909-1 | SW | NE | 29 | 38 | 8 | 4676430 | 590730 | Qbpb | Basaltic andesite | 51.76 | 0.99 | 18.65 | 4.73 | 3.69 | 0.14 | 4.52 | 9.62 | 3.50 | 0.83 | 0.33 | 1.22 | 99.98 |
| 980611-1 | NE | NE | 5 | 39 | 8 | 4673495 | 591205 | QTwb | Basalt | 48.52 | 1.08 | 17.54 | 5.02 | 5.24 | 0.17 | 7.19 | 11.14 | 2.84 | 0.17 | 0.12 | 0.92 | 99.95 |
| 980611-2 | NE | NE | 9 | 39 | 8 | 4672005 | 592805 | QTwb | Basalt | 48.26 | 1.04 | 16.90 | 2.55 | 7.44 | 0.17 | 9.02 | 10.84 | 2.64 | 0.15 | 0.10 | 0.97 | 100.08 |
| 980922-1 | SW | SE | 33 | 38 | 8 | 4674070 | 592435 | QTwb | Basalt | 47.07 | 0.99 | 16.82 | 4.20 | 5.42 | 0.16 | 9.49 | 10.01 | 2.40 | 0.15 | 0.11 | 3.72 | 100.54 |
| 980922-2 | — | NE | 33 | 38 | 8 | 4675080 | 592305 | QTwb | Basalt | 48.51 | 1.06 | 17.44 | 3.04 | 6.73 | 0.17 | 8.00 | 11.11 | 2.84 | 0.16 | 0.12 | 0.72 | 99.90 |
| 95-52 | SW | SE | 16 | 39 | 7 | 4669180 | 582830 | Tb | Basalt | 51.53 | 0.94 | 17.85 | 3.26 | 4.70 | 0.14 | 6.25 | 10.98 | 2.91 | 0.57 | 0.22 | 0.70 | 100.05 |
| 95-63 | SW | SW | 36 | 39 | 7 | 4664420 | 586630 | Tbke | Basalt | 48.69 | 1.11 | 16.62 | 1.49 | 7.98 | 0.16 | 9.08 | 11.84 | 2.64 | 0.11 | 0.06 | 0.66 | 100.44 |
| 95-65 | SE | NW | 26 | 39 | 7 | 4666530 | 584990 | Tbke | Basalt | 50.23 | 0.81 | 16.96 | 2.00 | 6.42 | 0.15 | 9.81 | 10.39 | 2.61 | 0.37 | 0.12 | 0.69 | 100.56 |
| 95MH-47 | SW | SW | 36 | 39 | 7 | 4664500 | 586780 | Tbke | Basalt | 47.78 | 0.95 | 17.69 | 2.87 | 6.34 | 0.16 | 8.59 | 11.53 | 2.60 | 0.11 | 0.07 | 0.68 | 99.37 |
| 95MH-49c | SE | SE | 35 | 39 | 7 | 4664205 | 586330 | Tbke | Basalt | 47.82 | 1.00 | 17.95 | 2.17 | 7.33 | 0.15 | 8.58 | 11.14 | 2.63 | 0.11 | 0.06 | 0.93 | 99.87 |
| 95MH-61 | NW | NW | 35 | 39 | 7 | 4665540 | 585020 | Tbke | Basalt | 49.32 | 0.81 | 17.19 | 1.95 | 6.38 | 0.15 | 9.36 | 10.54 | 2.60 | 0.34 | 0.12 | 0.79 | 99.55 |
| 95MH-75 | SE | SW | 36 | 39 | 7 | 4664180 | 587070 | Tbke | Basalt | 47.97 | 0.98 | 18.14 | 5.19 | 4.60 | 0.16 | 7.65 | 11.57 | 2.61 | 0.11 | 0.06 | 1.08 | 100.12 |
| 95MH-77 | SE | SW | 36 | 39 | 7 | 4664800 | 587180 | Tbke | Basalt | 47.68 | 0.99 | 17.53 | 1.37 | 7.66 | 0.16 | 8.92 | 11.35 | 2.44 | 0.22 | 0.06 | 1.49 | 99.87 |
| 980826-1 | SW | NW | 26 | 39 | 7 | 4666560 | 584970 | Tbke | Basalt | 49.32 | 0.80 | 16.63 | 2.52 | 6.25 | 0.16 | 10.21 | 10.02 | 2.48 | 0.32 | 0.13 | 1.21 | 100.05 |
| 980826-2 | NW | SW | 26 | 39 | 7 | 4666370 | 585145 | Tbke | Basalt | 49.58 | 0.82 | 17.15 | 3.01 | 5.42 | 0.16 | 9.15 | 10.51 | 2.68 | 0.33 | 0.15 | 0.86 | 99.82 |
| 981104-4 | NW | NE | 35 | 39 | 7 | 4665620 | 585945 | Tbke | Basalt | 50.14 | 0.86 | 16.94 | 3.07 | 5.66 | 0.16 | 9.02 | 10.33 | 2.74 | 0.40 | 0.14 | 0.73 | 100.19 |
| 95MH-84 | SE | NE | 34 | 39 | 7 | 4665210 | 584600 | Tpt | Basaltic andesite | 52.93 | 0.98 | 17.82 | 3.87 | 4.18 | 0.14 | 5.36 | 8.84 | 3.67 | 0.97 | 0.35 | 0.95 | 100.06 |
| 95MH-30 | SW | SW | 34 | 39 | 7 | 4664330 | 583590 | Tcm | Basaltic andesite | 54.20 | 1.07 | 18.18 | 2.86 | 5.01 | 0.14 | 3.91 | 7.93 | 3.91 | 1.26 | 0.33 | 1.02 | 99.82 |
| 95MH-4 | NW | NE | 33 | 39 | 7 | 4665400 | 582770 | Tcm | Basaltic andesite | 53.35 | 0.98 | 17.60 | 3.10 | 4.86 | 0.13 | 5.56 | 8.63 | 3.69 | 1.06 | 0.34 | 0.55 | 99.85 |
| 95MH-49a | SE | SE | 35 | 39 | 7 | 4664200 | 586330 | Tcm | Basaltic andesite | 52.60 | 1.13 | 18.13 | 2.97 | 5.78 | 0.15 | 5.10 | 8.09 | 3.57 | 0.90 | 0.35 | 1.00 | 99.77 |
| 95MH-68 | SW | SW | 35 | 39 | 7 | 4664280 | 585360 | Tcm | Basaltic andesite | 53.56 | 1.06 | 17.90 | 2.15 | 6.02 | 0.14 | 4.95 | 8.07 | 3.51 | 1.16 | 0.35 | 1.05 | 99.92 |
| 95MH-69 | SE | SW | 35 | 39 | 7 | 4664400 | 585680 | Tcm | Basaltic andesite | 53.02 | 1.08 | 17.83 | 2.30 | 6.24 | 0.15 | 5.45 | 8.12 | 3.48 | 1.09 | 0.33 | 0.82 | 99.91 |
| 981104-1 | SW | SW | 34 | 39 | 7 | 4664350 | 583360 | Tcm | Basaltic andesite | 53.42 | 1.05 | 18.33 | 3.22 | 4.65 | 0.13 | 4.50 | 8.11 | 3.81 | 1.20 | 0.36 | 0.94 | 99.72 |

* Samples 990121-4 and 990125-5 are field-split duplicates taken in adjacent Howard Bay quadrangle for isotopic dating.

→ percent, trace elements in parts per million (ppm). XRF analyses provided by the laboratory of S.A. Mertzman at Franklin and Mar-

| $Fe_2O_3T$ | Rb | Sr | Y | Zr | V | Ni | Cr | Nb | Ga | Cu | Zn | Co | Ba | La | Ce | U | Th | Sc | Pb | Yb | Hf | Ta | Nd | Sm | Eu | Tb | Lu |
|---|---|---|---|---|---|---|---|---|---|---|---|---|---|---|---|---|---|---|---|---|---|---|---|---|---|---|---|
| 11.55 | 2.8 | 369 | 27 | 103 | 221 | 132 | 269 | 4.2 | 18.1 | 52 | 84 | 43 | 175 | 8 | 17 | <0.5 | 0.6 | 27 | 6 | — | — | — | — | — | — | — | — |
| 10.91 | 5.0 | 434 | 28 | 135 | 206 | 90 | 165 | 9.7 | 18.6 | 64 | 75 | 35 | 283 | 15 | 26 | <0.5 | 0.6 | 24 | 5 | — | — | — | — | — | — | — | — |
| 10.89 | 3.2 | 423 | 30 | 135 | 210 | 100 | 188 | 9.2 | 18.8 | 56 | 78 | 39 | 458 | 16 | 28 | <0.5 | 1.2 | 27 | 5 | — | — | — | — | — | — | — | — |
| 11.31 | 4.1 | 403 | 31.7 | 137 | 221 | 100 | 187 | 9.8 | 19.8 | 61 | 81 | 41 | 427 | 15 | 26 | <0.5 | 2.5 | 29 | 5 | — | — | — | — | — | — | — | — |
| 8.26 | 14.3 | 595 | 19 | 106 | 178 | 64 | 85 | 5.5 | 18.4 | 60 | 75 | 27 | 421 | 12 | 29 | <0.5 | 0.8 | 20 | 7 | — | — | — | — | — | — | — | — |
| 8.23 | 11.6 | 662 | 12.4 | 106 | 179 | 62 | 101 | 5.7 | 20.5 | 58 | 78 | 26 | 468 | 14 | 27 | 0.8 | 1.6 | 21 | 7 | — | — | — | — | — | — | — | — |
| 8.07 | 13.1 | 651 | 13.5 | 105 | 176 | 61 | 99 | 5.4 | 20.3 | 58 | 76 | 26 | 437 | 12 | 32 | 1.4 | 3.4 | 21 | 7 | — | — | — | — | — | — | — | — |
| 9.09 | 10.2 | 561 | 18 | 75 | 165 | 109 | 225 | 3.8 | 17.0 | 44 | 65 | 32 | 328 | 11 | 20 | <0.5 | 1.8 | 20 | 4 | — | — | — | — | — | — | — | — |
| 8.83 | 9.3 | 775 | 19 | 97 | 239 | 35 | 73 | 6.2 | 19.7 | 88 | 85 | 28 | 509 | 20 | 33 | <0.5 | 2.4 | 25 | 6 | — | — | — | — | — | — | — | — |
| 10.84 | 2.6 | 306 | 25 | 66 | 242 | 123 | 229 | 1.8 | 16.3 | 91 | 71 | 45 | 144 | 3 | 14 | <0.5 | <0.5 | 30 | 3 | — | — | — | — | — | — | — | — |
| 10.82 | 2.8 | 274 | 23 | 55 | 223 | 148 | 270 | 1.9 | 16.5 | 86 | 66 | 43 | 155 | 5 | 13 | <0.5 | <0.5 | 27 | 4 | — | — | — | — | — | — | — | — |
| 10.22 | 2.0 | 256 | 21 | 55 | 214 | 163 | 297 | 1.9 | 14.9 | 85 | 71 | 44 | 84 | 3 | 9 | <0.5 | 0.7 | 29 | 3 | — | — | — | — | — | — | — | — |
| 10.52 | 2.8 | 308 | 23 | 58 | 223 | 129 | 201 | 2.2 | 17.0 | 77 | 71 | 43 | 113 | 4 | 9 | 0.5 | <0.5 | 29 | 4 | — | — | — | — | — | — | — | — |
| 8.48 | 7.2 | 821 | 15.2 | 80 | 227 | 39 | 118 | 4.4 | 18.8 | 33 | 69 | 28 | 278 | 11 | 37.2 | 1.6 | 2.4 | 31.1 | 8.4 | — | — | — | — | — | — | — | — |
| 10.36 | 2.4 | 358 | 24.6 | 54 | 245 | 136 | 291 | 3.5 | 17.7 | 120 | 65 | 41 | 75 | 4.2 | 6.8 | 1 | 2.1 | 35.1 | 5.1 | — | — | — | — | — | — | — | — |
| 9.13 | 4.5 | 524 | 18.1 | 53 | 202 | 183 | 465 | 3.7 | 17.5 | 77 | 64 | 36 | 181 | 6.6 | 20.6 | 0.7 | 0.7 | 27.7 | 5.1 | — | — | — | — | — | — | — | — |
| 9.92 | 2.7 | 298 | 22.6 | 50 | 210 | 156 | 213 | 3.5 | 17 | 96 | 65 | 42 | 65 | 3.1 | 4 | 0.7 | 1.8 | 29.9 | 6.6 | — | — | — | — | — | — | — | — |
| 10.32 | 2.5 | 309 | 22 | 56 | 218 | 160 | 210 | 3.4 | 17.6 | 97 | 65 | 41 | 69 | 2.3 | 3.1 | <.1 | 0.2 | 32 | 5.6 | 2.4 | 1.4 | <0.3 | 7 | 2.41 | 0.95 | 0.6 | 0.35 |
| 9.04 | 3.7 | 544 | 19.4 | 58 | 216 | 200 | 478 | 3.5 | 16.9 | 69 | 65 | 40 | 219 | 7.7 | 25.6 | 0.6 | 0.8 | 29.5 | 7.5 | 2.1 | 1.7 | <0.3 | 11 | 2.56 | 0.95 | 0.6 | 0.31 |
| 10.30 | 2.4 | 306 | 32.4 | 53 | 223 | 174 | 231 | 3.7 | 16.6 | 107 | 67 | 44 | 59 | 0.2 | 8.6 | 0.2 | 0.3 | 31.6 | 5.2 | — | — | — | — | — | — | — | — |
| 9.88 | 3.5 | 372 | 22.1 | 52 | 210 | 148 | 252 | 3.2 | 17 | 117 | 64 | 40 | 54 | 4.7 | 6.2 | 0.9 | 0.6 | 31.5 | 4.9 | — | — | — | — | — | — | — | — |
| 9.47 | 4.0 | 453 | 19 | 62 | 198 | 177 | 482 | 2.7 | 15.9 | 60 | 62 | 39 | 212 | 10 | 19 | 0.5 | 1.3 | 25 | 5 | — | — | — | — | — | — | — | — |
| 9.03 | 3.6 | 492 | 20 | 66 | 205 | 193 | 486 | 2.4 | 15.8 | 84 | 63 | 39 | 216 | 9 | 21 | <0.5 | 0.6 | 28 | 4 | — | — | — | — | — | — | — | — |
| 9.36 | 5.5 | 483 | 23 | 71 | 214 | 167 | 481 | 3.1 | 16.5 | 79 | 61 | 40 | 196 | 7 | 15 | <0.5 | 1.3 | 29 | 5 | — | — | — | — | — | — | — | — |
| 8.52 | 8 | 1,039 | 14.3 | 100 | 199 | 55 | 109 | 7 | 20.9 | 64 | 75 | 23 | 557 | 15.6 | 53.7 | 0.9 | 2.4 | 23.6 | 9.1 | — | — | — | — | — | — | — | — |
| 8.43 | 17.3 | 841 | 28.4 | 133 | 186 | 26 | 56 | 8.2 | 21.5 | 86 | 75 | 19 | 623 | 23.9 | 47.4 | 1 | 2.5 | 0.8 | 11.4 | — | — | — | — | — | — | — | — |
| 8.50 | 10.4 | 975 | 15.4 | 107 | 196 | 70 | 120 | 6.8 | 20.7 | 67 | 77 | 24 | 557 | 23.4 | 57.5 | 1.3 | 1.9 | 20.7 | 12.3 | — | — | — | — | — | — | — | — |
| 9.39 | 11.3 | 683 | 20.6 | 115 | 187 | 71 | 130 | 7.1 | 20.5 | 78 | 78 | 25 | 477 | 18.4 | 41.1 | 1.1 | 2.4 | 19.9 | 11.7 | 2.09 | 2.8 | <0.3 | 18 | 4.13 | 1.25 | 0.6 | 0.32 |
| 8.84 | 13.6 | 666 | 25 | 126 | 195 | 60 | 106 | 7.3 | 19.7 | 76 | 81 | 25 | 470 | 17.7 | 42.6 | 1.8 | 0.8 | 23.5 | 11.9 | — | — | — | — | — | — | — | — |
| 9.23 | 12.1 | 674 | 20.5 | 114 | 190 | 76 | 134 | 7.3 | 19.4 | 72 | 79 | 25 | 445 | 14.6 | 43 | 0.8 | 1.4 | 22.1 | 10.8 | — | — | — | — | — | — | — | — |
| 8.39 | 14.8 | 895 | 27 | 128 | 185 | 47 | 83 | 7.0 | 20.0 | 70 | 76 | 25 | 682 | 28 | 44 | 1.7 | 2.3 | 20 | 7 | — | — | — | — | — | — | — | — |

*(Continued on next page)*

Table 2, continued. Note that table extends across two pages. ➝

| Sample no. | ¼ | ¼ | Sec. | T.(S.) | R.(E.) | UTM N | UTM E | Unit | Lithology | $SiO_2$ | $TiO_2$ | $Al_2O_3$ | $Fe_2O_3$ | FeO | MnO | MgO | CaO | $Na_2O$ | $K_2O$ | $P_2O_5$ | LOI | Total |
|---|---|---|---|---|---|---|---|---|---|---|---|---|---|---|---|---|---|---|---|---|---|---|
| 980723-1 | SE | NW | 22 | 39 | 7 | 4668170 | 583910 | Tbis | Basalt | 51.07 | 0.92 | 16.93 | 4.02 | 4.58 | 0.15 | 6.90 | 10.53 | 2.87 | 0.53 | 0.22 | 0.91 | 99.63 |
| 980817-1 | SW | SW | 23 | 39 | 7 | 4667435 | 584965 | Tbis | Basalt | 51.44 | 0.92 | 17.75 | 4.65 | 3.50 | 0.14 | 5.85 | 10.76 | 3.00 | 0.57 | 0.23 | 1.00 | 99.81 |
| 980826-3 | SE | NE | 27 | 39 | 7 | 4666680 | 584680 | Tbis | Basalt | 50.57 | 0.94 | 18.02 | 3.88 | 4.38 | 0.15 | 6.30 | 11.12 | 2.92 | 0.39 | 0.25 | 1.17 | 100.09 |
| 980827-1 | NW | SW | 25 | 39 | 7 | 4666470 | 586675 | Tbis | Basalt | 51.48 | 0.93 | 18.04 | 3.03 | 5.08 | 0.14 | 6.17 | 10.37 | 2.96 | 0.57 | 0.24 | 1.30 | 100.31 |
| 981104-3 | SW | SW | 24 | 39 | 7 | 4667350 | 586840 | Tbis | Basalt | 51.40 | 0.88 | 17.71 | 3.32 | 4.80 | 0.15 | 6.36 | 10.69 | 2.91 | 0.51 | 0.20 | 1.11 | 100.04 |
| 95-64 | SW | NE | 35 | 39 | 7 | 4665160 | 585840 | Tham | Basaltic andesite | 53.12 | 1.11 | 17.69 | 2.15 | 6.38 | 0.15 | 5.75 | 8.21 | 3.56 | 0.96 | 0.37 | 0.64 | 100.09 |
| 95-66 | NW | NW | 35 | 39 | 7 | 4665610 | 585340 | Tham | Basaltic trachy-andesite | 51.81 | 1.16 | 18.16 | 6.54 | 2.63 | 0.15 | 4.48 | 8.28 | 3.75 | 1.35 | 0.47 | 1.30 | 100.08 |
| 98-95 |  | SW | 36 | 39 | 7 | 4664470 | 586970 | Tham | Basaltic trachy-andesite | 52.27 | 1.10 | 17.46 | 3.48 | 4.95 | 0.15 | 5.13 | 8.11 | 3.75 | 1.44 | 0.48 | 0.72 | 99.04 |
| 95MH-45 | NE | NW | 35 | 39 | 7 | 4665580 | 585560 | Tham | Basaltic andesite | 52.82 | 1.09 | 17.83 | 2.17 | 6.37 | 0.15 | 5.60 | 8.17 | 3.63 | 0.85 | 0.33 | 0.55 | 99.56 |
| 95MH-46 | SE | NE | 35 | 39 | 7 | 4664920 | 586270 | Tham | Basaltic trachy-andesite | 51.88 | 1.14 | 18.27 | 6.04 | 2.78 | 0.14 | 4.45 | 8.25 | 3.72 | 1.34 | 0.45 | 1.54 | 100.00 |
| 95MH-62 | NW | NW | 35 | 39 | 7 | 4665580 | 585170 | Tham | Basaltic trachy-andesite | 53.05 | 1.13 | 17.48 | 3.64 | 4.50 | 0.14 | 4.71 | 7.99 | 3.71 | 1.71 | 0.49 | 0.79 | 99.34 |
| 980715-1 | SE | SW | 36 | 39 | 7 | 4664480 | 587050 | Tham | Basaltic andesite | 51.67 | 1.18 | 17.23 | 4.33 | 4.09 | 0.15 | 5.89 | 8.08 | 3.69 | 1.07 | 0.43 | 2.61 | 100.42 |
| 990119-1 | NW | NE | 28 | 39 | 7 | 4666980 | 582900 | Tham | Basalt | 51.06 | 0.89 | 17.28 | 3.65 | 4.76 | 0.17 | 6.82 | 10.89 | 2.95 | 0.60 | 0.21 | 0.78 | 100.06 |
| 990119-2 | NE | SE | 27 | 39 | 7 | 4666350 | 584700 | Tham | Basalt | 50.77 | 0.90 | 17.32 | 3.90 | 4.44 | 0.16 | 7.05 | 10.89 | 2.91 | 0.56 | 0.22 | 0.76 | 99.88 |
| 980609-2 | NE | SW | 12 | 39 | 7 | 4671040 | 587010 | Tba | Basaltic andesite | 53.08 | 0.98 | 18.03 | 1.58 | 6.79 | 0.15 | 5.30 | 8.13 | 3.52 | 0.89 | 0.27 | 1.13 | 99.85 |
| 980609-3 | NE | SW | 18 | 39 | 8 | 4669710 | 588600 | Tba | Basaltic andesite | 54.79 | 1.02 | 17.55 | 2.64 | 5.23 | 0.14 | 4.11 | 7.33 | 3.88 | 1.31 | 0.55 | 1.00 | 99.55 |
| 980609-4 | NE | SW | 18 | 39 | 8 | 4669795 | 588605 | Tba | Basaltic andesite | 54.53 | 1.01 | 17.78 | 3.72 | 4.24 | 0.14 | 3.84 | 7.24 | 3.90 | 1.31 | 0.53 | 1.13 | 99.37 |
| 980827-4 | NW | SE | 24 | 39 | 7 | 4668000 | 587705 | Tba | Basaltic andesite | 54.65 | 1.04 | 17.85 | 3.48 | 4.68 | 0.13 | 3.89 | 7.31 | 3.96 | 1.30 | 0.53 | 1.09 | 99.91 |
| 980827-5 | NE | SW | 13 | 39 | 7 | 4669670 | 587090 | Tba | Basaltic andesite | 54.10 | 1.01 | 17.79 | 2.87 | 5.05 | 0.14 | 4.19 | 7.66 | 3.86 | 1.29 | 0.52 | 0.88 | 99.36 |
| 981013-1 | SW | NE | 18 | 39 | 8 | 4670195 | 589220 | Tba | Basaltic andesite | 51.93 | 1.11 | 17.77 | 2.83 | 6.24 | 0.16 | 5.67 | 8.06 | 3.74 | 0.98 | 0.52 | 0.74 | 99.75 |
| 981013-3 | NW | NE | 19 | 39 | 8 | 4668820 | 589330 | Tba | Basaltic andesite | 54.57 | 1.00 | 17.84 | 2.79 | 5.07 | 0.15 | 4.11 | 7.60 | 3.84 | 1.38 | 0.51 | 0.81 | 99.67 |
| 981120-1 | NW | SW | 31 | 38 | 8 | 4674350 | 588340 | Tba | Basaltic andesite | 53.49 | 0.99 | 17.88 | 2.83 | 5.25 | 0.14 | 5.68 | 8.30 | 3.61 | 0.72 | 0.21 | 0.99 | 100.09 |
| 990121-1 | NE | SW | 24 | 38 | 7 | 4677460 | 586955 | Tba | Basaltic andesite | 52.00 | 1.08 | 19.55 | 3.26 | 5.10 | 0.17 | 4.97 | 7.95 | 3.71 | 0.51 | 0.25 | 1.46 | 100.01 |
| 990121-2 | SE | NE | 25 | 38 | 8 | 4676250 | 587730 | Tba | Basaltic andesite | 52.65 | 1.18 | 18.56 | 3.07 | 5.84 | 0.15 | 4.95 | 7.95 | 4.05 | 0.78 | 0.34 | 0.38 | 99.90 |
| 95-1 | NW | SW | 29 | 39 | 8 | 4666240 | 590160 | Tbaa | Basaltic andesite | 52.41 | 0.91 | 17.63 | 3.60 | 4.82 | 0.13 | 6.24 | 8.17 | 3.56 | 0.84 | 0.21 | 1.72 | 100.24 |
| 980827-3 | SW | SE | 19 | 39 | 8 | 4667690 | 589010 | Tbaa | Basaltic andesite | 54.40 | 0.85 | 18.04 | 2.94 | 4.57 | 0.12 | 4.84 | 8.76 | 3.76 | 0.89 | 0.20 | 1.10 | 100.47 |

| $Fe_2O_3T$ | Rb | Sr | Y | Zr | V | Ni | Cr | Nb | Ga | Cu | Zn | Co | Ba | La | Ce | U | Th | Sc | Pb | Yb | Hf | Ta | Nd | Sm | Eu | Tb | Lu |
|---|---|---|---|---|---|---|---|---|---|---|---|---|---|---|---|---|---|---|---|---|---|---|---|---|---|---|---|
| 9.11 | 8.5 | 567 | 24 | 94 | 237 | 63 | 184 | 3.5 | 16.5 | 42 | 69 | 31 | 250 | 17 | 25 | <0.5 | 1.5 | 31 | 6 | — | — | — | — | — | — | — | — |
| 8.54 | 6.8 | 753 | 18 | 92 | 225 | 41 | 84 | 4.2 | 16.9 | 88 | 72 | 31 | 276 | 10 | 31 | <0.5 | 1.3 | 30 | 6 | — | — | — | — | — | — | — | — |
| 8.75 | 3.7 | 785 | 19 | 91 | 243 | 38 | 83 | 3.8 | 17.4 | 75 | 68 | 28 | 433 | 17 | 31 | <0.5 | 1.4 | 32 | 6 | — | — | — | — | — | — | — | — |
| 8.68 | 5.1 | 728 | 20 | 92 | 217 | 38 | 102 | 3.9 | 17.9 | 77 | 64 | 28 | 366 | 16 | 34 | <0.5 | 1 | 29 | 6 | — | — | — | — | — | — | — | — |
| 8.66 | 6.7 | 600 | 21 | 89 | 203 | 49 | 159 | 3.3 | 18.2 | 75 | 63 | 29 | 245 | 13 | 27 | <0.5 | 2 | 29 | 5 | — | — | — | — | — | — | — | — |
| 9.24 | 12.2 | 674 | 18.8 | 112 | 193 | 78 | 137 | 7.2 | 19.1 | 66 | 78 | 26 | 457 | 15.9 | 42.8 | 1.2 | 1 | 23.4 | 9.3 | — | — | — | — | — | — | — | — |
| 9.46 | 9 | 1149 | 17 | 141 | 186 | 66 | 95 | 8.5 | 21.5 | 66 | 87 | 25 | 786 | 24.8 | 70.5 | 0.8 | 1.9 | 23.9 | 10.9 | — | — | — | — | — | — | — | — |
| 8.98 | 14.1 | 1025 | 21.7 | 155 | 185 | 65 | 103 | 8.6 | 21.0 | 76 | 85 | 24 | 696 | 26 | 62 | 0.7 | 1.6 | 22 | 11 | — | — | — | — | — | — | — | — |
| 9.25 | 9.6 | 681 | 18.7 | 112 | 170 | 81 | 142 | 6.6 | 19.9 | 52 | 77 | 26 | 467 | 15 | 44.5 | 1.1 | 1.2 | 23.2 | 9.3 | — | — | — | — | — | — | — | — |
| 9.13 | 8.5 | 1150 | 17.3 | 143 | 182 | 66 | 89 | 8.4 | 21 | 66 | 86 | 24 | 766 | 26.5 | 73.5 | 1.1 | 3 | 24.6 | 10.6 | — | — | — | — | — | — | — | — |
| 8.64 | 19.5 | 1326 | 16 | 144 | 167 | 57 | 79 | 7.7 | 21.2 | 91 | 76 | 21 | 928 | 26.7 | 76.6 | 0.7 | 3 | 22.8 | 11.8 | — | — | — | — | — | — | — | — |
| 8.88 | 11.7 | 844 | 21 | 123 | 184 | 94 | 145 | 9.2 | 18.9 | 62 | 82 | 31 | 447 | 18 | 41 | <0.5 | 1 | 22 | 7 | — | — | — | — | — | — | — | — |
| 8.94 | 8.8 | 561 | 20.1 | 81 | 215 | 69 | 230 | 3.4 | 18.3 | 64 | 68 | 32 | 279 | 10 | 21 | 0.7 | 2 | 30 | 5 | — | — | — | — | — | — | — | — |
| 8.83 | 6.1 | 563 | 19.8 | 81 | 216 | 69 | 236 | 3.7 | 18.5 | 67 | 66 | 32 | 272 | 13 | 23 | 0.8 | 2.7 | 31 | 5 | — | — | — | — | — | — | — | — |
| 9.13 | 10.9 | 603 | 27 | 88 | 198 | 61 | 81 | 4.6 | 18.0 | 75 | 78 | 31 | 409 | 16 | 26 | <0.5 | 1.2 | 23 | 7 | — | — | — | — | — | — | — | — |
| 8.45 | 14.1 | 708 | 24 | 169 | 165 | 42 | 40 | 9.9 | 18.7 | 60 | 85 | 23 | 748 | 22 | 42 | 1 | 1.1 | 20 | 9 | — | — | — | — | — | — | — | — |
| 8.43 | 14.2 | 704 | 26 | 170 | 174 | 42 | 46 | 9.9 | 18.7 | 79 | 86 | 25 | 587 | 22 | 47 | <0.5 | 0.6 | 23 | 10 | — | — | — | — | — | — | — | — |
| 8.69 | 12.5 | 712 | 25 | 168 | 162 | 37 | 48 | 9.7 | 19.4 | 79 | 73 | 21 | 609 | 25 | 46 | <0.5 | 1 | 20 | 9 | — | — | — | — | — | — | — | — |
| 8.48 | 11.8 | 731 | 24 | 164 | 171 | 42 | 53 | 9.5 | 18.8 | 88 | 80 | 24 | 556 | 23 | 51 | <0.5 | 1.3 | 21 | 9 | — | — | — | — | — | — | — | — |
| 9.76 | 10.1 | 765 | 22 | 127 | 193 | 70 | 86 | 7.6 | 19.3 | 166 | 85 | 31 | 487 | 14 | 40 | <0.5 | 0.8 | 20 | 15 | — | — | — | — | — | — | — | — |
| 8.42 | 13.5 | 719 | 25 | 165 | 177 | 40 | 70 | 9.6 | 19.5 | 66 | 83 | 24 | 614 | 23 | 49 | <0.5 | 1.4 | 19 | 9 | — | — | — | — | — | — | — | — |
| 8.66 | 9.5 | 567 | 22 | 94 | 182 | 100 | 144 | 4.2 | 17.5 | 72 | 71 | 29 | 382 | 12 | 17 | <0.5 | 1.6 | 21 | 6 | — | — | — | — | — | — | — | — |
| 8.93 | 4.6 | 641 | 29.7 | 110 | 174 | 69 | 75 | 5.2 | 21.7 | 55 | 77 | 30 | 495 | 13 | 29 | 1.2 | 1.9 | 23 | 7 | — | — | — | — | — | — | — | — |
| 9.56 | 7.2 | 723 | 21.4 | 88 | 199 | 47 | 72 | 4.9 | 20.5 | 69 | 76 | 29 | 364 | 9 | 28 | <0.5 | 2.2 | 23 | 5 | — | — | — | — | — | — | — | — |
| 8.96 | 9.4 | 762 | 12 | 62 | 195 | 120 | 148 | 4.6 | 19.1 | 69 | 77 | 30 | 312 | 7.2 | 26.4 | 2 | 1.2 | 23.5 | 6.5 | — | — | — | — | — | — | — | — |
| 8.02 | 8.4 | 755 | 15 | 73 | 202 | 31 | 56 | 3.3 | 19.9 | 92 | 65 | 24 | 294 | 13 | 19 | <0.5 | 0.5 | 20 | 5 | — | — | — | — | — | — | — | — |